Highlights

Context-Aware Quantitative Risk Assessment Machine Learning Model for Drivers Distraction

Adebamigbe Fasanmade, Ali H. Al-Bayatti, Jarrad Neil Morden, Fabio Caraffini

- A novel multiclass driver distraction risk assessment model to use during a journey.
- The model categorises the driver on a risk matrix as safe, careless, or dangerous.
- Each event is associated with a severity level used to predict distraction.
- Real-world data from the Field Operation Test (TeleFOT) validate the model.

Context-Aware Quantitative Risk Assessment Machine Learning Model for Drivers Distraction

Adebamigbe Fasanmade[a], Ali H. Al-Bayatti[a], Jarrad Neil Morden[a], Fabio Caraffini[b,*]

[a]*School of Computer Science and Informatics, De Montfort University, Tthe Gateway, Leicester, LE1 9BH, England, UK*
[b]*Department of Computer Science, Swansea University, Bay Campus, Computational Foundry, Fabian Way, Swansea, SA1 8EN, Wales, UK*

Abstract

Risk mitigation techniques are critical to avoiding accidents associated with driving behaviour. We provide a novel Multi-Class Driver Distraction Risk Assessment (MDDRA) model that considers the vehicle, driver, and environmental data during a journey. MDDRA categorises the driver on a risk matrix as safe, careless, or dangerous. It offers flexibility in adjusting the parameters and weights to consider each event on a specific severity level. We collect real-world data using the Field Operation Test (TeleFOT), covering drivers using the same routes in the East Midlands, United Kingdom (UK). The results show that reducing road accidents caused by driver distraction is possible. We also study the correlation between distraction (driver, vehicle, and environment) and the classification severity based on a continuous distraction severity score. Furthermore, we apply machine learning techniques to classify and predict driver distraction according to severity levels to aid the transition of control from the driver to the vehicle (vehicle takeover) when a situation is deemed risky. The Ensemble Bagged Trees algorithm performed best, with an accuracy of 96.2%.

Keywords: Risk assessment, Decision support, Driver behaviour, Severity rating, Driver distraction

*Corresponding author
Email addresses: alex.fasanmade@dmu.ac.uk (Adebamigbe Fasanmade), alihmohd@dmu.ac.uk (Ali H. Al-Bayatti), jarrad.n.morden@dmu.ac.uk (Jarrad Neil Morden), fabio.caraffini@swansea.ac.uk (Fabio Caraffini)

1. Introduction

Since the emergence of new in-vehicle technologies, distracted drivers have become a central problem in road accidents. Intelligent Transportation Systems (ITS) continue to advance, allowing vehicles to take control to a semi-autonomous level 4 (or the level approved by the authorities) out of either necessity or driver choice. These factors combine to make drivers more reliant on having the vehicle perform in-vehicle tasks, increasing distraction and perpetuating risk. An Advanced Driving Assistance System (ADAS) can help prevent accidents by providing drivers with real-time risk assessments. The system uses contextual information—such as vehicle performance data and environmental conditions that directly impact driver safety—to evaluate driving situations both qualitatively and quantitatively. By analyzing these factors, ADAS can identify and mitigate potential risks before an accident occurs. For such systems to be effective in practice, they must provide not only accurate predictions but also interpretable outputs that support real-time decision-making by both human drivers and automated controllers [76].

The European Commission for Mobility and Road Transport Safety highlights that a significant proportion of road accidents occur when the driver is distracted. Common distractions include using handheld mobile devices, using the radio, eating, talking to passengers, smoking, and glancing at in-vehicle navigation systems [1]. According to Kulkarni and Shinde [2], in-vehicle interfaces can also overload the driver. Fatigued drivers pose an additional significant risk on the road. In recent years, the driver's eyes have become an efficient metric for measuring driver distraction, and the driver's ability to keep their eyes on the road is crucial. A statistical analysis by the Department for Transport shows that 383 of 1,456 fatal car accidents involved careless tendencies by pedestrians, while 110 were a result of reduced driver attention on the road [3]. Inexperienced drivers are another significant factor that has contributed to an increase in the number of road accidents. Skilled drivers adjust their driving strategy in time and predict different driving scenarios [4], unlike younger and inexperienced drivers' whose higher crash-incidence is attributed to low cognitive ability [5] and loss of attention due to distraction [6].

Modeling risk mitigation is challenging because official accident reports often lack clear data. This stems from two main issues: countries may use

different definitions of what constitutes a distraction, or some countries may not collect this data at all [8]. Driver distraction can be influenced by situational factors, which represent a significant gap in the available mechanisms that accommodate the context-aware risk model. The model should be concise enough with the ability of intelligent image recognition to detect and form a risk matrix to profile drivers into distraction classifications. This can reduce the occurrence of an accident by a significant margin.

The importance and urgency of driving risk mitigation techniques to prevent driving behaviour-related accidents is well established in the literature base [9, 10, 11, 12, 13, 14]. For a false-proof robust alert system, the precise classification of driving behaviour is needed. However, to the best of our knowledge, the current models lack the complexity, the rigidness, a synthesized dataset, an increased focus on a particular perspective (*i.e.* vehicle, driver, or environment), detection of false-positive classes, and therefore suffer from low accuracy.

Drivers can be classified into three groups: safe, careless, and dangerous. Capturing driver behaviour is crucial to risk mitigation, and developing context-aware ADAS may influence the risk levels and prevent accidents. However, such systems must ensure fairness by avoiding biases that could result from disproportionate weighting of environmental factors over driver behaviors, or vice versa. A robust risk assessment model should provide equitable evaluations across different road types, weather conditions, and driver demographics, while maintaining sensitivity to genuine safety risks [78]. Real-time novel risk assessment is essential for timely intervention.

This study makes key contributions to the field via:

- The development of a definition of an adaptive severity level for driver distraction.
- A frame-by-frame analysis of driver behaviour severity level in an ADAS.
- A proposed model for characterizing driver behaviour considering contextual factors such as speed, acceleration, and surrounding vehicles.
- The development of the MDDRA model for driving behaviour and its evaluation using machine learning (ML).

The following sections of the paper are structured accordingly.

- Section 2 presents the background of risk assessment related to driver's distraction and a detailed literature review on driver distraction.

- Section 3 describes the methodology of the MDDRA model, including a rigorous risk assessment.
- Section 4 presents the experiments and procedures, dataset, and technical setup.
- The findings and discussions of the experimental procedures are presented in Section 5.
- Finally, Section 6 concludes and suggests future work.

The literature review in Section 2 reveals that existing driver distraction models lack comprehensive context integration, employ binary classification with fixed thresholds, and provide reactive rather than predictive interventions. To address these limitations, we develop MDDRA using the TeleFOT naturalistic driving dataset, which provides synchronised driver, vehicle, and environmental data. Our methodology (Section 3) adopts a Dynamic Bayesian Network to integrate multi-domain inputs into continuous severity scores, enabling graduated interventions based on context-aware risk assessment. Section 4 describes our experimental validation through correlation analysis, regression testing, and machine learning classification to identify optimal algorithms for real-time deployment.

2. Literature review on drivers' distraction

2.1. Risk assessment for driver's distraction

Risk assessment can be defined as the process of evaluating the adverse effects of a natural phenomenon, activity, or substance [15]. Berdica stated that risk constitutes the likelihood and probability of an incident occurring [16, 17]. One approach to quantifying vehicle crash risk in bad weather uses a relative risk ratio. However, this method requires large datasets of weather-related crashes [18]. A more popular alternative is the risk matrix approach, which combines both the probability and consequences of potential accidents [16]. A risk matrix can be used to determine the level of driving risk. Most risk indicators for driver distractions are based on crash data. However, this approach has a fundamental flaw: it models risk assessment using post-crash data, making it a reactive strategy rather than a preventive one. According to Cai et al. [19], drivers' subjective assessment of driving risks - particularly those related to various weather scenarios - is consistent with collision-based

studies. In [19], the authors assume that the driver's perceived risks are consistent with the actual crash statistics, especially for incidences related to rainy conditions. Various factors can impact driving capability; these can be extracted from the driving context (i.e., from the driver, vehicle, and environment) and include weather conditions, road, speed, manoeuvres, pedestrians, driver state, and braking. However, adequate data and facilities to ensure the development and implementation of an efficient and robust risk assessment model for the driving context remain lacking. In response to this, this paper proposes using data from the TeleFOT Naturalistic Driving Study (NDS), which provides comprehensive monitoring of the environment, vehicle, and driver behavior. The proposed approach uses the following mathematical model:

$$C_i = \sum_{j=1}^{J} (x \cdot X_{i,j} \cdot \beta_j) + \varepsilon_i, \quad C_i = 1, 2 \ldots, M \tag{1}$$

where C_i denotes a discrete model-dependent variable that represents the level of a distraction impact on driving. This variable's various impact levels include minor impact, overall impact, profound impact, and disastrous impact. The i included in this variable represents the i^{th} driver with non-observable ε_i variables, including the volume of traffic, vehicle type, road type, and rain intensity. A non-observable variable is selected to fit a logistic distribution for generating a continuous latent variable C_i denoting the influence on driving.

Another proposed approach is the Rank Order Cluster Analysis, which sorts driving risk R_i in ascending order, as indicated by $R_1, R_2, R_3, \ldots, R_n$. Consideration of categories (G), including $R_i, R_{(i+1)}, \ldots, R_j$ and satisfying $j > i$ can be denoted as $G = \{i, i+1, \ldots, j\}$. Consequently, the diameter $D(i, j)$ of G is calculated from the equation:

$$D(i, j) = \sum_{t=i}^{j} (R_t - R_G)^2, \tag{2}$$

where R_G represents the mean driving risk, and the driving hazard is seg-

mented into k segments expressed as:

$$\begin{aligned} G_1 &= \{i_1, i_1 + 1, \ldots, i_2 - 1\}, \\ G_2 &= \{i_2, i_2 + 1, \ldots, i_3 - 1\}, \\ &\vdots \\ G_k &= \{i_k, i_k + 1, \ldots, i_{k+1} - 1\} \end{aligned} \tag{3}$$

Where the variable i satisfies the following condition:

$$1 = i_1 < i_2 < \cdots < i_k < i_{k+1} = n + 1. \tag{4}$$

There is also a minimal loss function with a recursion relationship represented by the equation:

$$L[b(n,k)] = \sum_{t=1}^{k} D(i_t, i_{t+1} - 1) \tag{5}$$

Where $b(n,k)$ denotes a special function returning a classification method based on the values of n and k. This function appears in the recurrence relation for the minimal loss function formulated in Equation 6 below,

$$L\left[b(n,k)_{k \le j \le n}\right] = \min_{k \le j \le n} \left\{L[P(j-1, k-1)] + D(j,n)\right\}, \tag{6}$$

where $P(n,k)$ denotes the method to minimise the loss function; if the values of n and k are given; $P(n-1, k-1)$, with different descriptions depicts the optimal driving risk categories. However, our proposed model assumes that driving is a discrete and time-series event; therefore, it takes the risk in the previous frame to compute the severity level of driving risk in the current frame. We further consider the sequence of occurrence and the duration of the distracted driving event in computing risk. We address the limitations, thereby enhancing our proposed model.

2.2. Face Orientation

Dong et al. [20] measure driver fatigue based on physiological features, including facial expression and eye activity, as well as the number of times that drivers touch their faces. Assuming that when drivers are tired they exhibit less frequent head motions, it is possible to measure driver fatigue based on the frequency of face turns during a journey. The starting duration depends on the deduction from a consecutive number of frames. Hu et al. [21]

state that careless driving is a significant cause of road accidents and tracked driver behaviour using face orientation and facial features taken from infrared images. However, the study uses a singular type of driver distraction, which represents a significant limitation.

Sato et al. [22] infer driver distraction and concentration states using driver body information states. They assessed near misses when drivers approached an intersection. Time series data on different eye-gaze movements and face orientations before the collision or near-miss were logged. Rasouli et al. [23] analyzed pedestrian behaviour at crossing points under various weather conditions and road types. Their findings show the vital significance of the head orientation of pedestrians before their crossing intention. Pedestrians assess traffic dynamics (such as vehicle speed) and crosswalk characteristics (such as width) to inform their crossing decisions. Their demographic characteristics further influence this behavior even after they have indicated their intention to cross. The result showed an interrelation in the contextual elements, with one factor potentially decreasing or increasing the influence of other factors.

Fasanmade et al. [24] use multi-class distraction to classify driver distraction into severity levels using drivers' physiological features. The approach involved the use of an image-processing rule-based fuzzy logic system. They found that a combination of face orientation and eye glance increases the degree of driver distraction. Their results further showed that driver distraction could transition from careless driving to dangerous driving when a certain threshold is reached and when multi-class distraction occurs.

2.3. Hand State

Hands are vital in driving tasks, such as steering and changing gears. During operation, the state of hands is even more critical in a changing context. Monitoring hand state is consequently crucial to the prevention of accidents. Das et al. [25] describe a naturalistic driving study to detect drivers' hands using bounding boxes and hand annotation. The validation involved checking for false positives that may arise due to illumination conditions, no-hand objects of similar colour, occlusion, and truncation. Aggregate Channel Features (ACF) was used as the detector and the hand detector's accuracy was measured using precision-recall (PR) to evaluate the parameter performance. The initial results suffered from missed detections and false positives, although a cross-dataset comparison yielded better accuracy.

Dong et al. [26] state that fatigued drivers assume more comfortable hand positions on the steering wheel. However, Carsten and Brookhius [75] noted that the impact of cognitive distraction on driving performance differs from that of visual distraction. Specifically, visual distraction adversely impacts a driver's steering ability and lateral vehicle control, particularly car following.

Le et al. [27, 28] use a novel multiple-scale region-based fully convolutional neural network (MSRFCN) for human region detection in illuminated and low-resolution conditions. They further use a pre-trained network called the "Oxford" hand dataset and compare it with several hand detection approaches. The proposed MSFRCN algorithm has an Average Precision (AP) and Average Recall (AR) of 95.1% and 94.5%. It brings an improvement in the AP and AR of 7% and 13%, respectively, to classify both the left and right hands.

2.4. Eye Glances

According to an eye-tracking study by French carmaker Peugeot, during a one-hour trip in urban traffic, car drivers take their eyes off the road for a total of about two miles. The study involves several drivers on 25 parallel six-mile drives utilising special driver-mounted glasses to investigate where their eyes alighted when operating a range of SUV vehicles. Results revealed drivers had eyes off the road for about 7% of the trip [29].

Yuan et al. [30] suggest an approach to classify existing driving situations and forecast off-road vehicle situations using a Hidden Markov Model (HMM). The experiment is performed using a driving simulator analysis involving 26 driver participants in three driving scenarios: rural, urban, and motorway environments. Three different occlusion durations ($0\,s$, $1\,s$, and $2\,s$) are added to measure the eyes-off-road period durations. The results reveal that existing driving situations can be optimally defined using glance position sequences, with up to 89.3% accuracy [80]. The motorway is the most distinguishable with over 90% precision. In driver's eyes-off-road period estimation, using HMM-based algorithms with two inputs (namely look duration and look position sequences), yields an accuracy rate of 92.7%. Vehicles of 42 newly approved adolescent drivers are fitted with sensors, accelerometers, and Global Positioning Systems (GPS) to collect data continuously for 18 months period. Crash and near-crash (CNCs) situations were reported through the investigation of significantly elevated gravitational force incidents [81]. Analysis of the video assigns 6 seconds previous to each CNC, and random samples of non-CNC road fragments are coded for the period

of eye-glances off the front road and occurrence of secondary mission participation. The likelihood (odds ratio) of crashes and near-crashes (CNCs) due to eye-glance behavior is determined by comparing two scenarios: (1) the frequency and duration of eyes-off-road glances during secondary tasks immediately before CNCs, versus (2) the frequency and duration of eyes-off-road glances during normal driving segments without CNCs. The crash incidence improved with the period of the single-most prolonged glimpse during all secondary tasks (OR = 3.8 for $> 2\,s$) and wireless secondary task presence (OR = 5.5 for $> 2\,s$). The single-most extended glimpse offers an improved constant estimation of an accident's likelihood than absolute eyes off the forward roadway [31].

2.5. Road Type (Urban, Highway)

In [32], Doshi et al. develop an algorithm that includes critical vehicle data, such as the brake switch status, throttle position, and wheel speed. It also uses the inputs to calculate several parameters, namely shifts per given time interval, throttle variations, mean velocity, and acceleration. The resulting parameters help the algorithm to identify the road type on which the assigned vehicle was traveling. This road identification process is achieved through parameter comparisons with reference values that defined various road types [71]. The algorithm also identified the driver type using driver inputs, such as gear shift patterns and the driver's handling of the brake and accelerator pedals. Doshi et al.'s algorithm attained a Receiver Operating Characteristic (ROC) value of 85% accuracy in road-type identification.

The behavioural analysis on road rage in China by Chai et al. [33] reports an inverse proportionality between cases of road rage and lane number on a given road. In other words, with fewer lanes, there are more incidences of road rage. The study reveals that road rage also increases with an increase in the number of non-motorized vehicles. Road rage generally involves fewer trucks, although more trucks are involved in road rage on highways and daytime driving, which leads to fewer incidences involving non-motorized vehicles. A limitation of the study is its small sample size and lack of demographic and environmental variables, necessitating a more detailed analysis in the future.

To characterise road types and measure the degree of driver aggression, Messeguer et al. [34] design and implement a neural network-based algorithm to assist drivers by pointing out unacceptable driving behaviours. Their test results prove the precise ability of neural networks in the classification of driver and road types. With contextual information playing a critical role in

the accurate performance of various road classification and driver distraction identification algorithms, useful contextual information collection is vital.

Rakotonirainy et al. [35] and Khan [36] propose a context-aware system for the real-time collection and analysis of contextual information related to a vehicle, the immediate environment, and the driver. The system also gathered information from questionnaires. A Bayesian network model is employed to analyse contextual information through a learning model. This facilitates the observation and prediction of a driver's future moves 7[82]. The model attains a comparable accuracy in predicting future driver behaviours and warning other road users. However, the system is too complicated to implement in real life and false alerts remain a key problem of this system [46].

Methods for recognising and classifying road traffic accident severity play an essential role in understanding accidents, their causes, and possible mitigation strategies. To that effect, Jianfeng et al. [37] design a set theory-based accident recognition and classification method that supports vector machines. Their model employs rough set theory in calculating the significance of the driving environment, road, vehicle, and human attributes, and the results demonstrated the model's ability to improve recognition accuracy and reduce computational workloads. The study is limited in that it does not consider human physical behaviour, such as the driver's face orientation [83].

2.6. Weather

The travel weather warning system (TWWS) by Cai et al. [19] is similar to a Road Weather Information System (RWIS) for sharing weather safety information and disseminating safety warnings to drivers. This system is made up of risk estimate models that were based on extensive weather-related crash data. Weather-related data are collected using questionnaires, wherein drivers identify the various risks encountered while driving under different driving conditions. The severity of each type of weather is measured on a four-point scale ranging from slight to catastrophic. Metrics such as the intensity of rain and traffic volume are also considered.

Malin et al. [38] state that rainy weather is a significant factor in traffic accidents, with the risk of accidents increasing under poor road weather conditions.

Sherretz and Farhar [39] report a positive linear correlation between rainfall and the frequency of road traffic crashes. Bergel-Hayat et al. [40] also

revealed a significant correlation between the aggregate number of traffic accident injuries and weather variables. They observe that the correlation between these two parameters varies depending on road type.

Brodsky and Hakkert [41] propose measuring the risk of a road accident during rainy weather. Their method shows a drastic rise in road traffic accident injuries during rainy weather compared to dry weather. The increased dangers under wet conditions that follow a long dry season are well known to drivers, as was found by Knapper [42].

2.6.1. Speed

Maintaining the correct speed continues to be a challenge for many drivers. Drivers who violate driving rules, such as speeding, crash more often. Stradling and Auberlet [28, 43] show that vehicle trajectory variations may disclose valuable details on how spatial restrictions impact the behavior of drivers (e.g., lateral location and speed). Their findings reveal that while driving on the crest vertical curve measure, before encountering oncoming vehicles and narrower lane width, the lateral location variability is more significant; although this was reduced according to the perceptual procedure used. Another study investigated the impact of multiple factors, such as image size, speed, the shape of the road, driving experience, and gender, on the drivers' perception of their speed.

Wu et al. examine the most miniature image scale (38% of the actual field of view) in [44] and find that speed calculations are the most reliable. The driving velocity is gradually undervalued as the image scale grows. Participants with driving expertise correctly measured the driving speed on both wide and narrow roads. However, those without driving experience make more underestimates on broader roads. Furthermore, environmental conditions concerning speed performance have been highlighted by Bellis et al. [45]. They challenge the current policies and suggest interventions through teaching drivers about the inverse illumination-speeding relationship and measuring how better vehicle headlights and intelligent road lighting can attenuate speed.

Real-world speeding and its association with illumination, an environmental property described as the incidence of luminous flux on a surface, has been examined in the literature. Manser and Hancock [47] address the need to ascertain whether visual patterns and wall tunnel texture impact driving performance since maintaining the correct speed continues to be challenging. The findings show that the relationship between drivers' speed and reaction

is impacted by the visual pattern and the tunnel wall texture.

2.7. Vehicle

Mishra and Baja [48] and Kamar and Patra [49] adopt ML approaches to predict the driving patterns of drivers and the impact on their social behaviour using CCTV cameras installed to monitor traffic. Their observations are carried out during the day, and the metrics for measurement are instances of traffic violations due to aggressive patterns.

Lee and Kum [50] propose a feature-based lateral position estimation algorithm that employs lateral positioning and stereo vision, irrespective of changes to viewpoints and obstructions, resulting from pixel-wise feature extraction. The algorithm extracts vehicle images through image filtering, and thresholding, and removes the ground portions from images captured by cameras. The algorithm's detection component consists of a deep convolutional neural network with a sped-up robust feature (SURF) to match successive image frames. They estimate the lateral position of ground points using an inverse perspective mapping algorithm (IPM). The testing and validation phases are carried out using urban roads and highways to attain zero mean error and a standard deviation of $0.25\,m$ in lateral position estimation.

[51] detected driver behaviour based on car-following behaviours, which can vary according to distraction, fatigue, drivers' habits, and surrounding traffic. They use on-road trajectory data obtained in Beijing, and distinctive driver states and car-following models are observed as metrics. This led to the prediction of the driver's velocity control with improved accuracy.

Mittal [52] used object detection and a faster R-CNN model to detect vehicles of different scales and sizes. An evaluation is performed using the $\text{FLIR}_{\text{ADAS}}$ dataset for both RGB and thermal images. Gong et al. [53] instead propose using the YOLOv3 algorithm to detect vehicles in thermal images, achieving a 65% higher accuracy and speed than the original YOLOv3-tiny.

2.7.1. Pedestrians

In [54] Kharjul et al. introduce an active protection automobile pedestrian identification device to minimise the amount and intensity of vehicle-pedestrian collisions. They present a pedestrian identification approach that segments pedestrian candidates in images. The method uses Ada-Boost and cascading algorithms to confirm whether each claimant is a pedestrian. The Support Vector Machine (SVM) is used as a final classifier which exploits the input features of grey images for training.

Taiwan and Yamada develop in [55, 56] a tool for calculating driver knowledge and behaviour concerning pedestrian positions at crosswalks and while crossing, especially at left and right turns at intersections. Their findings on an appraisal carried out using objective evidence of driving behaviour on public roads have also been published. In contrast, Rangesh et al. [57] examine the behaviour of pedestrians. In particular, from a solely vision-based point of view, they concentrate on detecting pedestrians engaging in secondary behaviours involving their mobile phones and other handheld multimedia devices. They propose a pipeline integrating articulated human pose prediction and gradient-based picture features to detect the presence/absence in either a pedestrian's hand. A belief network is used to encode knowledge from multiple streams and their dependency on each other. This network is then used to forecast a likelihood score that suggests pedestrians' engagement with their devices [77].

Phan et al. [58] focus on drivers' actions whenever a person emerges in front of their car. They used two static parameters-based methods, namely the Necessary Deceleration Parameter and Time-To-Collision, and compare them to the proposed approach. They also employ a Hidden Markov Model (HMM) to characterise driver knowledge and unawareness of pedestrians. Compared with the baseline algorithms, the outcome indicates a significant enhancement of the HMM-based process.

2.8. Illumination (Day, Night)

In [59], Clarke et al. observe that the rate and severity of road traffic accidents are influenced by driving. In their study, the visibility conditions under investigation include rainy and night driving, with the control test being dry daytime driving. Their findings on the increased rate and severity of crashes at night and during rainy weather match the conclusions of [60], where the risk of fatal crashes is shown to increase by a factor of four during night driving compared to daytime driving.

3. The Multi Class Driver Distraction Risk Assessment Model

Based on existing literature, we develop and test our hypothesis that driver behaviour based on driver distraction has different severity levels, which we define as 'safe', 'careless', or 'dangerous'.

We then justify the weighting metrics for the distractions present in the TeleFOT dataset [68]. The following observable parameters can characterise

signs of attention deficit and fatigue in the driver: PERCLOS (PERcentage of eye CLOSure, i.e., the percentage of the time the driver's eyes are closed) [61], turning the head to the left/right to the body, tilting the head forward relative to the body (the moment when the driver is "nodding off"), duration and frequency of blinking, and the degree of openness of the person's mouth (a sign of yawning). In particular, for PERCLOS, there was a discrete number of parameters defined, namely P70, which is the proportion of time for which the eyes were closed of at least 70%; P80, which is the proportion of time for which the eyes were closed of at least 80%; and EYEMEAS (EM), which is the mean square percentage of the eyelid closure rating [61]. Furthermore, general information describing a driver helps not only explicitly identify that driver among all other drivers who installed and used a particular monitoring software package but also helps to improve the search for and classification of drivers with similar characteristics (general patterns among groups would help to predict developing situations). This can be accessed via the database, with a weight coefficient applied since this is a "common" behaviour rather than an individual driver's behaviour. Ginting et al. [62] adopted a 5-point Likert scale to model anxiety about individual coronary heart disease at different levels. Lopez-Fernandez et al. [63] also used a scale in assessing problematic internet entertainment among adolescents. The scale adopted was a self-administered scale for measuring the behavioural addiction of online social network users and video gamers regarding the degree of severity. We formulated the distraction severity levels based on these using a 5-point Likert-type scale, as seen in Table 1, [64, 65, 66].

The proposed model considers the severity level of driver distraction based on an observation of their driving history. While this can be unpredictable, we analyse the driver's behaviour frame by frame to obtain fine-scale details. We take the following steps:

- Decompose the video to a frame-by-frame level.
- Study each frame to assess its severity level.
- Aggregate the previous severity level of frames to the current frame severity level.
- Provide a precise class of severity based on the calculated severity level.

In the following, we outline the essential aspects of our model for accessing the severity level of driver distraction. We acquired the knowledge and data

by observing and analyzing individual frames from the input source. We began by formulating the risk assessment based on driver behaviour according to $P = p_1, p_2, p_3, \ldots, p_n$, as described in Table 1. Each parameter P_i is characterized by some set of action $A = a_1, a_2, a_3, ;a_n$, with each action a_i having a weight W_i.

Table 1: The essential aspects of the proposed model for accessing the severity level of driver distraction. The maximum weight values are reported in boldface.

Parameter	**Action**	$\mathbf{W_i}$
State of Hand	Double hand	0
	Single hand	1
	No hands	**2**
Road Type	Urban	1
	Dual	2
	Highway	**3**
Face Orientation	On road	1
	Off-road	**2**
Illumination	Day	1
	Night	**2**
Eye Gaze	Eyes on road	0
	Eyes off-road	1
	Eyes shut	**2**
Weather	Dry	1
	Rain	2
	Snow	**3**
Manoeuvres	Stopped	0
	Turning	1
	Moving	**2**
Surroundings	Vehicle not present	0
	Vehicle present	**1**
Pedestrians	not present	0
	present	**1**

The next stage consists in identifying the severity levels, according to severity rates, respective colour for identification, and classification label to start with. For instance, if the severity is 0.0, the risk colour will be right green, this will be no distraction from the driver has been observed, and it

will have no impact on the driver's life. While, if the severity level is 0.9 or above, the risk colour will be red, and it will mean that a severe causality can be expected, and it is hazardous to keep driving. Table 2 provides these details along with the relevant consequences.

Table 2: Severity level, the risk colour and its impact on the consequences

Severity (0.0 - 1.0)	**Risk Color**	**Impact**	**Distraction**	**Consequences**
0.0	Light Green	No Impact	Safe	No distraction
0.1-0.25	Green	Slight Impact	Safe	Slight distraction
0.25-0.399	Yellow	Low	Safe	Noticeable distraction
0.4-0.599	Dark Yellow	Medium	Careless	distraction detected
0.6-0.79	Orange	High	Dangerous	Frequent distractions
0.8-0.9	Dark Orange	Very High	Dangerous	Casualty prone
0.9-1.0	Red	Extreme	Extremely Dangerous	Severe casualty Prone

3.1. Risk Assessment Matrix

An approach to the computation of risk assessment in a quantitative model uses a Risk Assessment (RA) Matrix's graphical tool. The risk matrix involves calculating the magnitude of the potential consequences scaled on the vertical axis (levels of probability) of these consequences occurring; technically, the probability of these consequences occurring on the horizontal axis. This facilitates an increase in the visibility of risk and impacts decision-making. The risk is computed by calculating the Consequence Likelihood of Occurrence Likelihood. Here, the likelihood depicts the probability of a driver's distraction being related to their context awareness. Consequences/Severity Level: The occurrence of multi-class context-aware distractions is classified into severity levels of distraction.

3.2. Probability

Probability is the measure of the likelihood that an event will occur. For example, there is a possible aggregation to measure the number of times a driver experiences a particular distraction during a driving course. The driver may be profiled according to the distraction severity level at the end of the driving course.

3.3. Likelihood

The likelihood levels can be described as frequency values (duration course) and state values (every frame). Four impact levels are considered in this paper: no impact, low impact, medium impact, and high impact. When an effect has no impact, the likelihood score is one, and the likelihood of that distraction observes no distraction or a distraction that has not currently occurred. When a slight distraction is detected, the impact is low, with a score of 2. A medium result is considered when a minor distraction has occurred, and the score is then set to 3; 4 implies a medium to significant distraction occurrence. More impacts can be seen in Table 3 below.

Table 3: Severity Risk Matrix, 5 continuous frames, progression of danger

Severity	**Severity values**				
Extreme	7	7	14	21	28
Very High	6	6	12	18	24
High	5	5	10	15	20
Medium	4	4	8	12	16
Low	3	3	6	9	12
Slight/Very low	2	2	4	6	8
No Impact	1	1	2	3	4

We propose using a weighted average of the parameters to compute the severity levels per frame, as depicted in Table 1–4. These weights are capped by the maximum number that a parameter can take. For example, we take "State of Hand" as a parameter and grade it as follows: 0 - double hands, 1 - single hand, 2 - no hands. If the value of a given frame for this parameter is x, then the weighted value is $x/2$ since the maximum value of this parameter can take 2. We generalise this for any parameter x_i with a maximum value m_i as Severity level $= \sum_{i=0}^{n} x_i/m_i$. Where n is the number of parameters in consideration.

3.4. Special considerations

To ensure the safety of drivers [67] developed a lane departure warning system based on image processing using a mono camera installed inside the car. A distinctive feature of the system is that it successfully processes several road conditions, including undesirable situations such as changing the width of the road lane, the radius of its curve, the direction of the road, and the

Table 4: Severity Risk Assessment Matrix

RA	Likelihood
1	No distraction is observed or occurred yet
2	A slight distraction has been observed
3	A minor distraction has occurred
4	A medium or major distraction has occurred

complete absence of a road surface. From this we gather that speed depends on the road type; hence, we multiply it by the weight of its road for speed. We considered road type in the UK as this conforms to the source of the dataset. For the metric of road types, we define the threshold according to the speed limit allowable on the road type, i.e., urban, single carriage, and motorway at 30 mph, 60 mph, and 70 mph, respectively. Furthermore, we define the following contextual data:

- Vehicle V and driver data with probabilities $P(V) = \{v_1, v_2, \ldots, v_m\}$
- Environment E and environmental data with probabilities $P(E) = \{e_1, e_2, \ldots, e_n\}$
- Speed a
- Probability of Surrounding $P(S)$
- Probability of Pedestrians $P(Pe)$

We formulate the following equations. The speed is computed as described in equation 7, for example, given that the national speed limit of the UK is 70 mph and the maximum road type weight and the score is 3:

Let the national speed limit of the UK be denoted by MaxSpeed = 70 mph, and let the maximum road type weight and score be denoted by MaxRoadType = 3. Then the speed on a given road can be computed as follows:

$$\text{Speed} = \frac{\text{MaxSpeed} \cdot \text{MaxRoadType}}{\text{RoadType}} \cdot \frac{1}{\frac{\text{RoadType}}{\text{MaxRoadType}}} \tag{7}$$

where *RoadType* is the numerical value representing the type of road, such that higher values indicate more challenging road conditions. The fraction

$\frac{RoadType}{MaxRoadType}$ adjusts the speed based on the road type so that the speed is reduced on more challenging roads.

We understand there are different data points in each frame; thus, the severity level of a given frame with k data points where severity (S^*) of a given frame is (fi):

$$S(f_i) = \frac{1}{k}\left(\sum_{i=0}^{m} P(V_i) + \sum_{j=0}^{n} P(E_i) + aP(S) + P(Pe)\right) \tag{8}$$

We now compute the aggregate severity (S^*) of a given frame (fi) given the last $i-t$ frames. This is achieved by taking the average of the current frame's severity score compared to the severity score of the last i-t frames:

$$S(fi) = \frac{1}{t}\left((S(fi) + \sum_{j=t}^{i-1} S(f_j)\right) \tag{9}$$

The verification and validation processes for the proposed model typically include both computational and physical aspects. To assess the degree of adequacy of the numerical modelling, the following steps can be performed: 1) Determine the order of convergence of numerical solutions in comparison with a numerical solution using a reduced number of parameters; and 2) assess the sensitivity of the sampling algorithm to various uncertainties, including parameter constraints, grid adaptation to real measurements and boundary conditions. Validation assumes a careful comparison of the numerical calculation results of the phenomenon under study with experimental data to obtain an answer to the question "is the numerical solution correct?". A comparative analysis of the model with all the conditions, including the uncertainties associated with missing parameters and boundary conditions from the real world and computational points of view, is carried out.

Select methods can be used for model validation purposes;

- The L2 Loss method evaluates the loss function to compute the squared error for each training dataset and returns the square of the differences between the actual and the predicted values, i.e. $L = (y - f(x))^2$.
- Errors (residuals) can be predicated via a cross-correlation test: *Are the residuals uncorrelated with the input?*

- The model can be applied to unseen data (cross-validation). This strategy may be helpful since it establishes the robustness of the proposed model. It can also provide the basis for the hybrid cross-correlation validation since there is a need to separately investigate how the inputs and outputs are correlated and how this correlation is affected by our modelling scheme;

- "Inverse Problem" approach, i.e., acquire a solution to the problem and solve the inverse case to obtain the output parameters. This will help to validate the assigned weight coefficients and the overall parameterisation scheme.

In our case, the reliability of our model is tested by performing a cross-correlation test to analyze the residuals. This is carried out on the data obtained over two separate datasets, with the analysis separately applied to the inputs and outputs.

4. Experimental Methods

A discrete-time model is proposed for the application of ML to detect the pattern in time-series driver distraction data. Consequently, we develop an adaptive model for the prediction of the driver's severity level based on distraction. The MDDRA model architecture illustrated in Figure 1 shows the state flow of the data and system modules that constitute the entire system.

The architecture follows principles of multi-source system integration similar to those employed in intelligent traffic monitoring systems [79], where computer vision, embedded sensors, and data processing subsystems are unified into a cohesive framework. However, our architecture is specifically designed for continuous risk assessment rather than discrete event detection, incorporating six interconnected states that enable real-time severity scoring and predictive vehicle takeover decisions. The key architectural novelty lies in the integration of temporal modeling (frame-by-frame progression), probabilistic inference (Dynamic Bayesian Network), and machine learning classification to transform multi-source raw data into actionable risk assessments with distinct severity levels.

The architecture is made up of six states, as described in the following subsections.

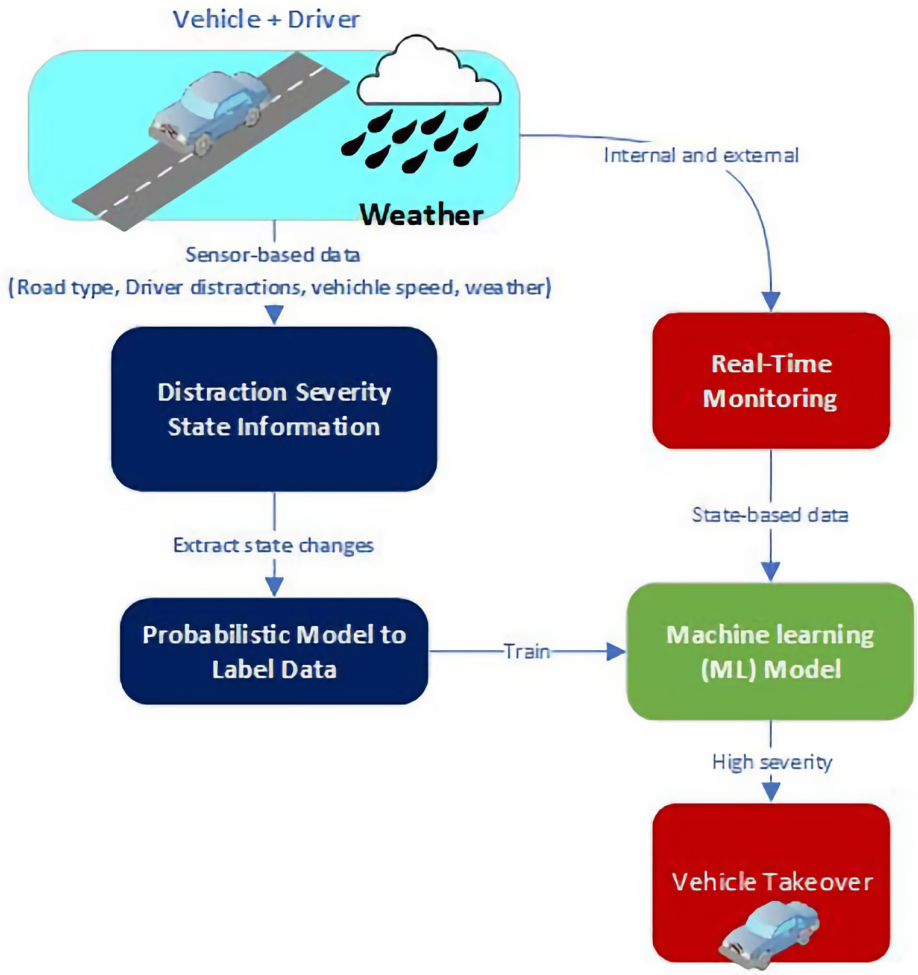

Figure 1: MDDRA Model Architecture

4.1. Driver and vehicle data collection

All required data are collected (from the vehicle and driver) using multiple sensors and video recorders. Sensor-based data are collected in real-time, including road type, driver movements, face and head direction, vehicle speed, weather, and the surrounding driving environment.

4.2. Object extraction

This architecture module extracts distraction state information (gaze at something else, Overspeed, etc.), including the changing state of the distrac-

tion, and feeds it into a probabilistic model for labeling.

4.3. Data labeling

The probabilistic model is further applied to the labeled extracted data, which is then used to train the system's core engine before the ML model is applied.

4.4. Real-time monitoring

Context-aware real-time data from the real-time driving video streams of the internal and external sensors of the vehicle are monitored. The data are further analyzed, and feature extraction of both the driver and vehicle state-based data is performed; this is then fed into the ML model.

4.5. Data Preprocessing

The TeleFOT dataset used in this study contained multimodal sensor recordings synchronised across in-vehicle and external cameras, accelerometers, and GPS modules. Prior to feature extraction, raw data were examined for completeness and signal quality. Instances with missing timestamps or corrupted sensor values below 0.5% of the total data were linearly interpolated to preserve temporal continuity. Sensor noise in the accelerometer and gyroscope channels was reduced using a fourth-order Butterworth low-pass filter with a 5 Hz cut-off frequency. Outliers caused by sudden signal spikes were detected through interquartile range analysis and replaced with the local mean of neighbouring samples. All numerical features were normalised to a $[0, 1]$ range to ensure equal scaling across predictors before training. Categorical variables, including road type and weather condition, were encoded using one-hot representation. The resulting cleaned dataset consisted of 264 labelled frame sequences, each annotated with synchronised driver, vehicle, and environmental attributes, forming the input for subsequent correlation, regression, and classification analyses.

4.6. ML model

The ML model takes in state-based data (eye gaze, state of hands, speed, face orientation, manoeuvre) and training datasets to predict the level of distraction. The resultant model is the probability of the occurrence of driver distraction in the current distraction frame state $P(C_{t+1} \mid S_{t+1})$, measured as the state transition from the previous frame state, denoted as $P(S_{t+1} \mid C_t)$. If the severity of distraction is high, vehicle takeover operations take effect.

4.7. Vehicle takeover

The severity informs the decision to perform a vehicle takeover of the distraction detected by the ML. If the distraction passes the threshold, i.e., transitions from careless to dangerous, then the decision for the vehicle to take over driving is triggered.

A Dynamic Bayesian network (DBN), as depicted in Figure 2, is an extension of a Bayesian network that uses the time (dynamic) concept in modeling sequential time-series observations. It also uses a probabilistic inference model in handling uncertain information. An acyclic graphic represents the conditional independent and latent temporal variables discretely and continuously. For this case, the inference from the DBN is derived from three key classes of nodes: driver features, distraction identifiers, and contextual data. These inputs are represented in this model by nodes such as the state changes of the driver, consisting of 5 central nodes: face orientation, speed, manoeuvres, eye gaze, and state of hands. The environmental changes node, consisting of road type, weather, and time of the day, forms part of the contextual input data into the model and data on pedestrians and the surrounding environment. The final input is the distraction identifier derived from the analysis of the driver features by a hybrid CNN-LSTM. The output of this acyclic graph is a severity score, which is the measure of the degree of the distraction of the driver extracted from the driver features and contextual information.

4.8. Dataset

The TeleFOT Naturalistic driving study dataset is a European TeleFOT [68]. The project was designed to enhance research on ITS [69, 70]. The experiment was conducted in the UK and involved 27 participants [70]. Each driving video consists of four video channels that monitor in-vehicle and out-vehicle parameters, including face orientation, eye gaze, and hand position. The dataset consists of time-series data, the camera is located inside the vehicle on the dashboard and on the passenger side of the vehicle, it also has two extra cameras to capture the environment as illustrated in Figure 3.

4.9. Probabilistic data model

We considered the driver distraction state's changes frame by frame, as depicted in Figure 2. Technically, our proposed Context-aware probabilistic model for severity classification can be described as the probability of the occurrence of driver distraction in the current frame state $P(C_{t+1} \mid S_{t+1})$

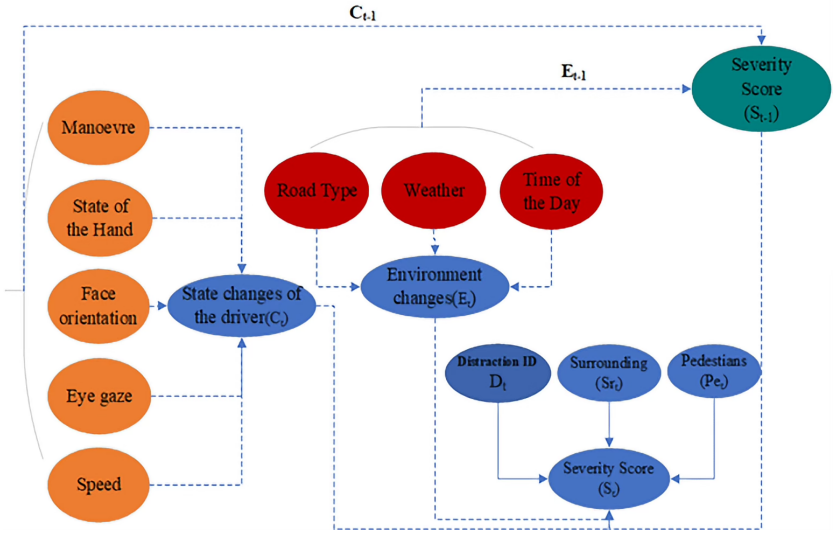

Figure 2: Context-aware Dynamic Bayesian Network for severity classification. **Nodes:** Orange nodes represent driver state changes: Manoeuvre, State of the Hand, Face Orientation, Eye Gaze, and Speed. Red nodes represent environmental state changes: Road Type, Weather, and Time of the Day. Dark blue nodes represent external contextual factors: Distraction ID, Surrounding vehicles (Sr), and Pedestrians (Pe). The central blue node integrates driver and environmental states, feeding into the Severity Score output (teal node). **Edges:** Solid arrows indicate probabilistic dependencies between variables. Dashed boxes delineate input domains. The network computes severity probability by combining temporal state transitions with multi-domain context (Equation 11).

from the previous frame state $P(S_{t+1} \mid C_t)$. So, there exists the probability of the occurrence of distractions in the environmental state $P(E_{t+1} \mid S_{t+1})$, if the current frame state S_{t+1} changes from the previous frame state S_t. The proposed extended dynamic Bayesian model includes several environmental variables such as road type, weather, and day. In order to compute the probability severity scores $P(S_{t+1} \mid C_{t+1}, E_{t+1}, Sr_{t+1}, Pe_{t+1}, S_t)$, we utilized the dynamic linear model 10 which is a combination of the state change of driver distraction C_{t+1}, environmental changes E_{t+1}, distraction identification D_{t+1}, pedestrians Pe_{t+1}, and surroundings Sr_{t+1}.

$$\begin{aligned} P(S_{t+1} \mid C_{t+1}, E_{t+1}, Sr_{t+1}, Pe_{t+1}, S_t) = \\ P(C_{t+1} \mid S_{t+1}) \cdot P(E_{t+1} \mid S_{t+1}) \cdot \\ P(Sr_{t+1} \mid S_t) \cdot P(Pe_{t+1} \mid S_{t+1}) \cdot \\ P(D_{t+1} \mid S_{t+1}) \cdot P(S_{t+1} \mid S_t) \end{aligned} \tag{10}$$

Figure 3: TeleFOT Dataset

4.10. Interdependencies Test

We can apply the developed interdependency test for road type and its impact on driving speed. For example, in Figure 4, the regression analysis coefficient is calculated as 0.529, implying a significantly positive relationship. We assume that the driver would drive within the UK speed limit. The dataset of the driver may be more biased towards a degree of severity compared to other databases. Thus, it is necessary to validate the model using a regression model to test the interdependencies. We perform a correlation analysis between driver distraction and the severity classification of the distraction. Also, we conduct a multi-linear regression analysis to estimate the influence of driver distraction on the degree of severity classification.

4.11. Data Normalisation

We log and normalize the vehicle's speed synchronously with the distraction state frame; thus, the time-series data of the vehicle are correlated at every frame. Subsequently, a regression analysis is conducted to validate our hypothesis. The severity level classification of the baseline drivers is likely to have a lower mean than experienced drivers. An additional regression analysis is performed using three categories of input variables: in-vehicle parameters, vehicle performance data, and environmental conditions. The analysis calculates mean values for these variables to establish a baseline safe severity

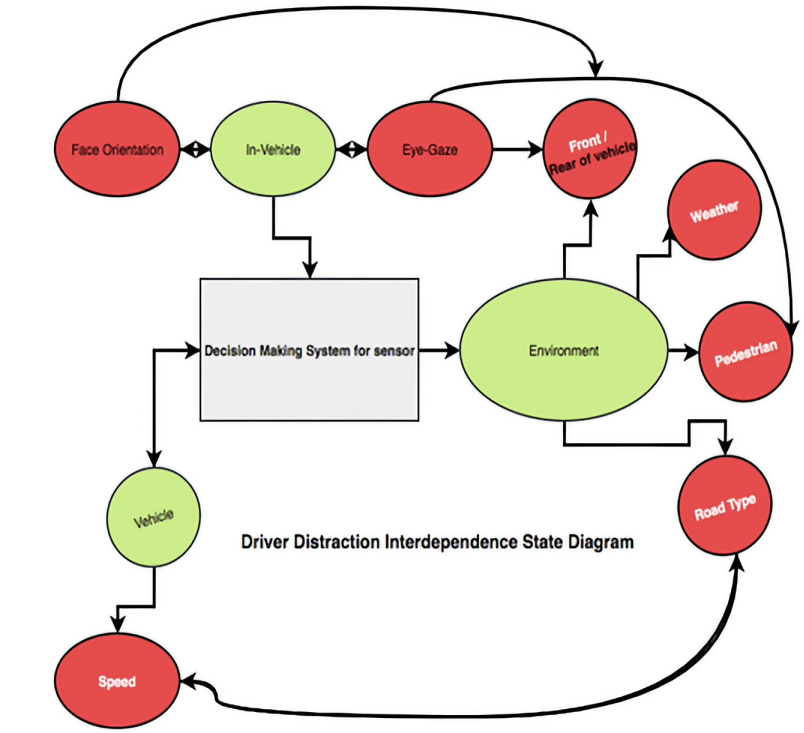

Figure 4: Distraction Interdependence State Diagram

level for typical drivers. Professional drivers are expected to maintain safety at severity levels above this baseline due to their training and experience. The severity level can be calculated at different temporal scales: instantaneous severity (per frame) or aggregated severity (averaged over time periods). Statistical analysis reveals that while all parameters contribute to determining whether driving behavior is safe, careless, or dangerous, two factors have the most substantial impact: (1) vehicle speed distribution throughout the journey, and (2) the interaction between road type and driver distraction severity level.

4.12. Results of the model validation procedure

To provide basic information about the variables in the dataset, the descriptive statistics for one of the simulated events (driver 1, event 1) are presented in Table 5. The mean, median, kurtosis, and skewness values are calculated by using equation (11) to (14).

$$\text{mean} = \frac{\text{Sum}(x)}{\text{Count}(n)} \tag{11}$$

$$\text{Median}(x) = \begin{cases} X\left[\frac{n}{2}\right] & \text{if } n \text{ is even} \\ \frac{X\left[\frac{n-1}{2}\right]+X\left[\frac{n+1}{2}\right]}{2} & \text{if } n \text{ is odd} \end{cases} \tag{12}$$

where X is an ordered list of values in the data set, and n denotes the number of values in the data set (count). For univariate data $y_1, y_2, \ldots, y_N$ the formula for skewness is:

$$g_1 = \frac{\frac{1}{N}\sum_{i=1}^{N}(y_i - \overline{y})^3}{S^3} \tag{13}$$

where $\overline{y}$ shows the mean, S is the standard deviation, and N is the number of data points. Note that in computing the skewness, the S is computed with N in the denominator rather than $N - 1$.

$$\text{kurtosis} = \frac{\frac{1}{N}\sum_{i=1}^{N}(y_i - \overline{y})^4}{S^4} \tag{14}$$

$$S = \sqrt{\frac{1}{N}\sum(y_i - \overline{y})^2} \tag{15}$$

The results of these metrics suggest that this is a symmetrical distribution. This reflects how the data were modeled. It would be valuable to deploy this model using real data from the video sensor to access the accurate distribution of parameters, such as face orientation and eye gaze, and then analyse the results.

To validate the model, its predictions are tested using correlation analysis. This technique is typically used to test relationships between quantitative or categorical variables. Correlation coefficients have a value between -1 and 1. A "0" value means that there is no relationship between the variables, while -1 or 1 means a perfect negative or positive correlation.

Table 6 showed that Surrounding (r = 0.44), State of Hand (r = 0.43), and Face Orientation (r = 0.42) were the strongest contributors to distraction severity, indicating that physical driver posture and environmental density have major influence on risk levels. Road Type (r = 0.36) and Maneuver (r = 0.32) showed moderate associations, while variables such as Weather, Time of Day, and Pedestrians exhibited weaker relationships (r ¡ 0.3). Speed

Table 5: Descriptive Statistics

Mean	0.513049625
Standard Error	0.007304311
Median	0.508023896
Standard Deviation	0.118456024
Sample Variance	0.01403183
Kurtosis	0.057262351
Skewness	0.217203269
Range	0.725482175
Minimum	0.162361126
Maximum	0.887843301
Sum	134.9320515
Count	263
Largest (1)	0.887843301
Smallest (1)	0.162361126
Confidence Level (95.0%)	0.014382625

Table 6: Correlation Coefficients

State of Hand	0.425847
Road Type	0.363796
Face Orientation	0.420461
Time of day	0.224532
Eye Gaze	0.296584
Weather	0.247372
Maneuver	0.323121
Speed	0.053056
Surrounding	0.441935
Pedestrians	0.255076

($r = 0.05$) showed almost no correlation with severity within this dataset and was therefore excluded from subsequent interpretive analysis. The model is also tested on multiple events, and the results demonstrate a consistent lack of correlation with velocity. This might indicate a need for a wider velocity span to be present in the dataset or, if this does not affect the results, better represent the model's influence.

4.13. Model Implementation Details

The Ensemble Bagged Trees classifier was implemented in MATLAB R2024a using the `fitcensemble` function with bagging as the ensemble method. Each ensemble consisted of 100 decision trees trained on bootstrapped subsets of the data to reduce prediction variance and enhance generalisation. The minimum leaf size for each tree was set to 8, and at each split, three predictors were randomly selected to ensure diversity among trees. Ten-fold cross-validation was employed to estimate out-of-sample accuracy, and model parameters were tuned through grid search to balance computational cost and predictive performance.

During training, the input feature set included state of hand, face orientation, eye gaze, vehicle speed, manoeuvre type, road type, weather condition, time of day, surrounding vehicles, and pedestrian presence. The response variable was the frame-wise distraction severity score obtained from the Dynamic Bayesian Network layer. Following training, the model produced class probabilities for the three severity categories: *safe*, *careless*, and *dangerous*. A decision threshold of 0.33 was applied for each class to maintain balanced sensitivity across the categories.

All statistical analyses and visualisations, including confusion matrices (Figure 10), scatter plots, and residual diagnostics (Figure 11), were generated using MATLAB's `confusion chart`, `resub Predict`, and plot Residuals functions. Computations were performed on an Intel Core i7 processor with 16 GB RAM and 4 GB GPU. The complete implementation and parameter configuration are available as supplementary material to facilitate reproducibility.

5. Results and Analysis

The implementation of our model and architecture in Figure 1 was carried out to determine which ML model will best predict driver distraction to aid in vehicle takeover decision-making. The results of the experiment were determined using different ML algorithms in the dataset to avoid bias. We analyse the scatter plot and the confusion matrix of the predicted class.

5.1. Interdependency Test using Regression Analysis

The regression analysis was performed on the following three context-aware characteristics:

1. The in-vehicle features related to the driver distraction such as hand moment, gaze;
2. The vehicle features such as vehicle speed, manoeuvres;
3. The environmental features such as pedestrians, vehicles, and weather.

The association and interdependencies between a pair of distractions need to be tested. We applied a regression to the prediction of driver distraction divided into severity levels. Here, we further tested the relationship between distractions by classifying distractions as either in-vehicle, context-aware, or environmental distractions.

5.1.1. Driver Distraction

Driver distraction features consist of state of hand, face orientation, and eye gaze. Figure 5 shows driver distraction, showing a strong relationship between eye gaze on the road (eye gaze 0), off-road face orientation and a single hand on the wheel, and having a high severity level of distraction leading to dangerous driving. Eyes closed, the orientation of the face on the road, and double hands-on wheel also significantly affect the severity score.

Table 7 presents the distractions in the vehicle with respect to the prediction of the severity score. Based on the P value of 0.758, the probability of the state of hands to predict the severity of distraction is low. The intercept of 0.529 suggests a relationship between the state of hands, face orientation, and eye gaze. The statistical predictors use the t-statistics and P-values of each distraction. The lower P-value of 0.249 for face orientation shows that this is a highly significant predictor of the severity score. The coefficient of determination is 0.005668.

Table 7: Human Distractions Regression Analysis

Intercepts	**Estimated**	**Std Error**	**T-Value**	**P Value**
State of Hand	0.015526	0.015526	34.080	0.758
Face Orientation	0.1–0.25	0.014414	−1.156	0.249
Eye Gaze	0.002045	0.008981	0.228	0.820
Intercept	0.529134	0.015526	34.080	<2e-16

5.1.2. Environmental Distractions

Figure 6 shows that dry weather, dual carriageway and a bright day produced the highest dangerous severity score, while rainy weather, double

Figure 5: Multiple regression analysis of in-vehicle driver behavioral parameters on severity score. **Variables:** State of Hand (x-axis: 0 = double hands on wheel, 1 = single hand on wheel, 2 = no hands on wheel); Eye Gaze (facet panels: 0 = eyes on road, 1 = eyes off-road, 2 = eyes shut); Face Orientation (color coding: purple circles and line = 0 [face oriented toward road], red circles and line = 1 [face oriented off-road]). **Output:** Severity Score (y-axis, continuous scale 0.2–0.8). **Visualization:** Each point represents a single frame observation. Linear regression lines (fitted separately for each Face Orientation category within each Eye Gaze facet) show predicted severity trends.

carriageway, and night produced a slightly more dangerous situation. Snowy conditions on the highway and at night had the highest degree of influence on the severity score.

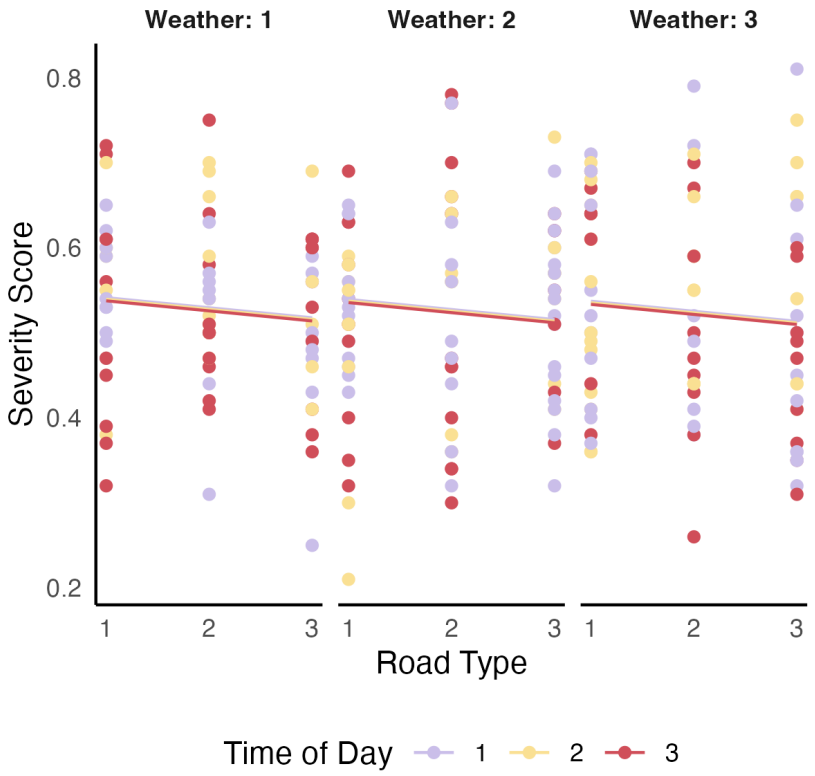

Figure 6: Environmental parameters regression on severity score. Road Type (x-axis: 1 = urban, 2 = dual carriageway, 3 = highway) versus Severity Score (y-axis, 0.2–0.85), faceted by Weather condition (1 = dry, 2 = rain, 3 = snow) and colored by Time of Day (purple = day, yellow = evening, red = night). Each point represents an individual observation; linear regression lines show fitted trends for each Time of Day within each Weather condition.

The results in Table 8 show how environmental distraction influence the prediction of the severity score.

The low P-value of 0.175 for the road type shows that the road type has a highly significant impact on the prediction. The environment intercept of 0.556982 showed a significant association between the severity score and the type of distraction road of the result, the time of day and the weather.

However, the lowest average P-value of 0.5897 was the lowest compared to the other distraction classifications. The least residual standard error of 0.1165, which is the smallest of all residual standard errors, indicates that this model best fits the data.

Table 8: Environment Regression Analysis

Intercepts	**Estimated**	**Std Error**	**T-Value**	**P-Value**
Road Type	−0.011838	0.008702	−1.360	0.175
Time of Day	−0.011848	0.008579	−0.215	0.830
Weather	−0.002086	0.009035	−0.231	0.818
Intercept	0.556982	0.031870	17.477	<2e-16

Figure 7 shows five instances of vehicle presence and pedestrian presence that result in a hazardous distraction classification, which means that if there are vehicles or pedestrians present in the surroundings, the chances of distraction by the driver are significant.

Table 9 presents the in-vehicle distractions to the prediction of the severity score. Based on the P-value of 0.532, the probability that the surroundings influence the prediction is low. The intercept of 0.529, which is significant, suggests a relationship between the surroundings and pedestrians. The statistical predictors use the t-statistics and P-values of each distraction. The lower P-value of 0.532 for the surroundings (vehicle presence) is a highly significant predictor of the severity score. However, the P-value of 0.830 for pedestrians suggests that there is no association between pedestrians and the severity score.

Table 9: External Distractions Regression Analysis

Intercepts	**Estimated**	**Std Error**	**T-Value**	**P-Value**
Surrounding	−0.009065	0.014502	−0.625	0.532
Pedestrians	0.003121	0.014487	0.215	0.830
Intercept	0.529157	0.013145	40.255	<2e-16

Vehicle distractions include manoeuvres and speed. Figure 8 shows the distraction within the speed range of 23 mph to 26.2 mph due to the high frequency of speed manoeuvres. There are a few outliers - defined as those points with either very high severity (> 0.79) at typical speeds or very low

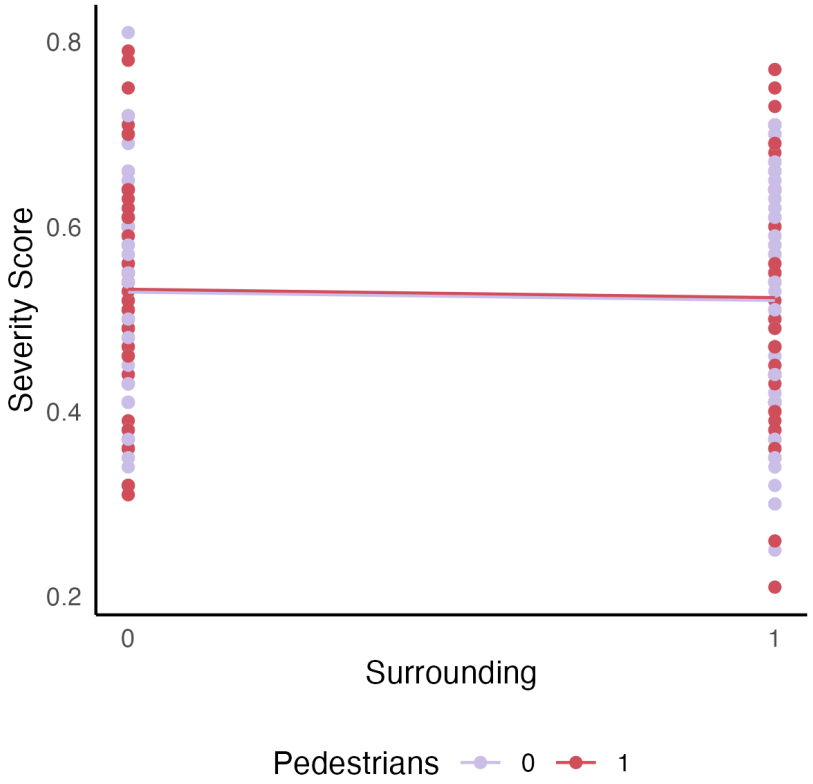

Figure 7: External contextual factors regression on severity score. Surrounding vehicles (x-axis: 0 = not present, 1 = present) versus Severity Score (y-axis, 0.2–0.85), colored by Pedestrian presence (purple = not present, red = present). Each point represents an individual observation; linear regression lines show fitted trends for each Pedestrian category.

severity (< 0.3) at extreme speeds - that are indicative of high levels of danger.

The results in Table 10 show the influence of vehicle distractions on the prediction of a severity score. Based on the p-value of 0.855, the probability that speed influences the prediction is low because the driver stays within the speed limit. However, during manoeuvres, there is a higher degree of significance. The intercept of 0.695812, which is highly significant, suggests a strong relationship between speed and manoeuvre. The statistical predictors use the t-statistics and P-values of each distraction. The lower P-value of 0.815 for manoeuvres shows that this is a highly significant predictor of the

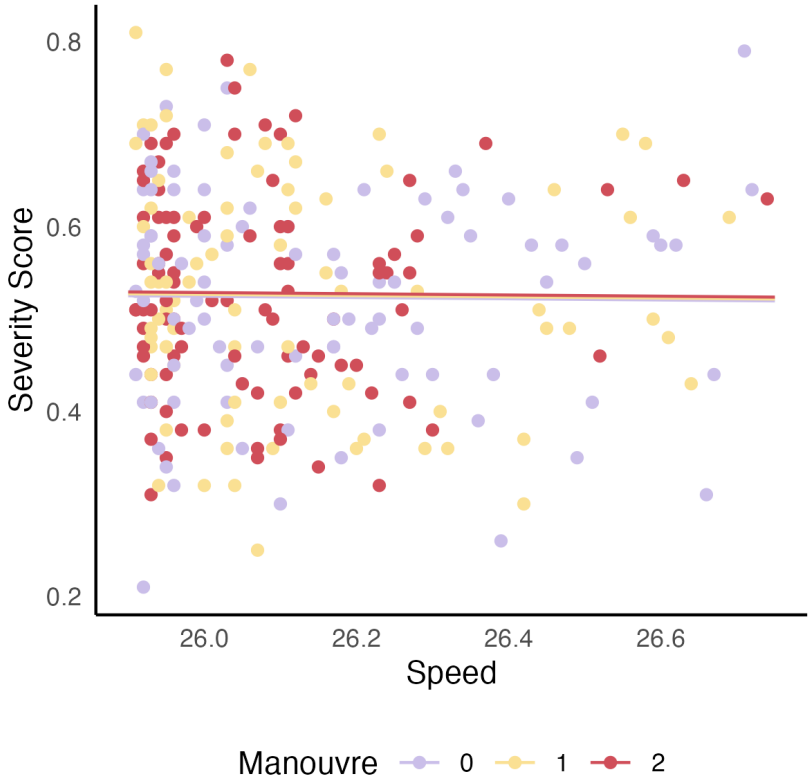

Figure 8: Vehicle dynamics regression on severity score. Speed (x-axis) versus Severity Score (y-axis, 0.2–0.85), colored by Manoeuvre type (purple = stopped, yellow = turning, red = moving). Each point represents an individual observation; linear regression lines show fitted trends for each Manoeuvre category.

severity score.

Table 10: Vehicle Distractions Regression Analysis

Intercepts	**Estimated**	**Std Error**	**T-Value**	**P-Value**
Speed	−0.009065	0.035983	−0.183	0.855
Manoeuvre	0.002050	0.008758	0.234	0.815
Intercept	0.695812	0.941042	0.739	0.460

In this case, the driver is tested with the previous severity score and the predicted actual severity score of the following video frame; in this experiment, the driver's overall performance is tested throughout the drive,

whereby there are a total of 262 frames, which is the equivalent of approximately 11 seconds. In Figure 9, we can assume that the driver has maintained a primarily constant careless driving behaviour. Our regression analysis results in a strong correlation between the previous severity score and the current severity score.

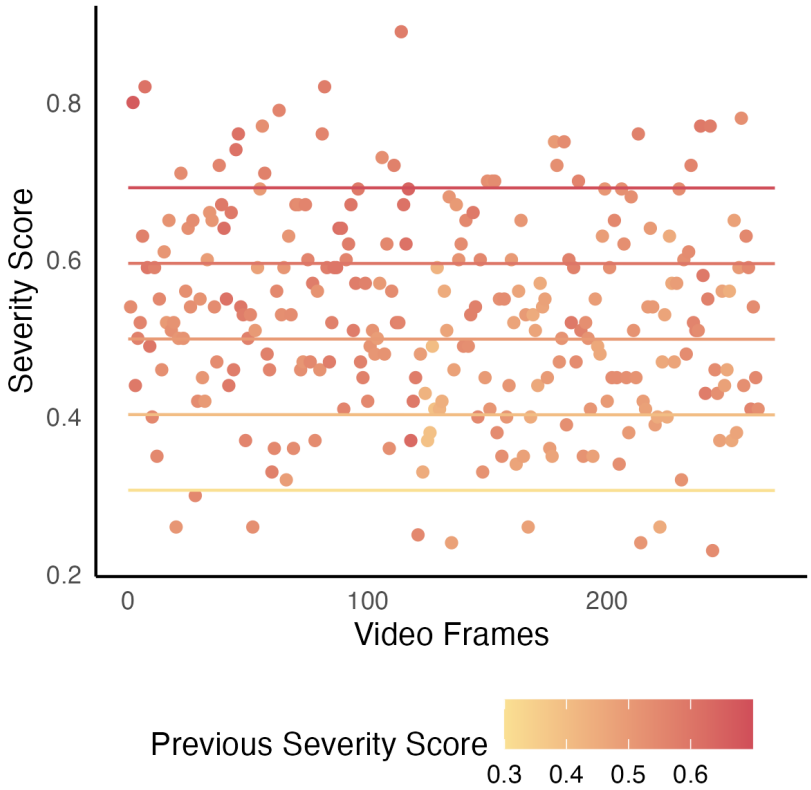

Figure 9: Temporal severity score progression across video frames. Video Frames (x-axis) versus Current Severity Score (y-axis, 0.2–0.95), colored by Previous Severity Score (gradient: yellow = 0.3, orange = 0.4–0.5, red = 0.6–0.7). Each point represents a frame observation; horizontal regression lines show fitted trends for discrete previous severity bins. Clear vertical stratification by color demonstrates strong temporal autocorrelation: frames with higher previous severity (dark red) maintain higher current severity, while lower previous severity (yellow-orange) maintains lower current severity.

Table 11 revealed that only the *Previous Severity Score* variable was statistically significant ($p = 1.8 \times 10^{-8}$), indicating a strong temporal dependency where the current frame severity depends heavily on the previous

frame's value. In contrast, *Video Frames* ($p = 0.990$) and the model intercept ($p = 0.845$) were not statistically significant, suggesting that the sequence index alone does not predict severity when prior frame information is included. These results imply that distraction severity evolves smoothly over time, and frame-to-frame continuity is the primary predictor within the regression model.

Table 11: Severity Score Regression Analysis

Intercepts	**Estimated**	**Std Error**	**T-Value**	**P-Value**
Video Frames	-1.329×10^{-6}	1.024×10^{-4}	-0.013	0.990
Previous Severity Score	9.618×10^{-1}	9.618×10^{-1}	5.812	1.8×10^{-8}
Intercept	1.828×10^{-2}	1.828×10^{-2}	0.196	0.845

5.2. ML Model

We implemented different ML models, such as discriminant, Nïve Bayes, SVM, K-Means Nearest Neighbour (KNN), and Ensemble ML. To better evaluate performance, the comparison of the classification results is shown in Table 12.

In Figure 10, the first two diagonal cells show the percentage of correct classification by the trained network. For example, 142 frames are correctly classified as careless. This corresponds to 99% of the 262 frames. Similarly, 80 cases are correctly classified as dangerous, which corresponds to 96% of all edges. Three dangerous and three safe instances are incorrectly classified, corresponding to 12% of all 264 frames in the data. Similarly, one of the careless structures is incorrectly classified, corresponding to 1% of all data. Out of 148 careless predictions, 99% are correct and 1% are wrong. Of the 80 dangerous predictions, 96% are correct and 4% are wrong. Of 35 safe cases, 92% are correctly predicted as safe, and 8% are correctly predicted as false.

5.2.1. Time Complexity

Safety in ITS is critical, and having a fast ML model to make an efficient decision is crucial for the safety of road users. Figure 11 refers to the amount of time it takes to train a model, make predictions, or perform other operations related to the learning process. The histogram of residual values displays the frequency distribution of the residuals in graph (a) indicates the distance between the observed prediction time from the mean of each classifier's total time for training. The significant residual value between -200

Table 12: Classification performances for the KNN, Discriminant, Naïve Bayes, SVM and Ensemble models.

Model	**Acc. %**	**Speed**	**T-Time**
Fine KNN	79.1	2700	4.4574
Medium KNN	78.3	2500	3.5617
KNN Coarse	59.3	2500	4.4974
KNN Cosine	80.6	2600	4.368
KNN Cubic	76.4	2000	4.239
KNN Weighted KNN	80.6	2500	3.975
Linear Discriminant	90.9	2700	3.5265
Quadratic Discriminant	82.9	2500	5.2346
Gaussian Naïve Bayes	93.2	3000	5.0814
Kernel Naïve Bayes	90.1	1500	5.9402
Linear SVM	92.0	2400	4.9151
Quadratic SVM	92.4	2300	4.8007
Cubic SVM	92.4	2300	4.6915
Fine Gaussian SVM	58.6	2200	5.7229
Medium Gaussian SVM	85.2	2100	5.5983
Coarse Gaussian SVM	77.2	2300	5.4722
Boosted Trees	58.6	3600	4.5331
Bagged Trees	96.2	1000	6.3019
Subspace Discriminant	92.4	780	6.8675
Subspace KNN	79.8	600	6.7319
RUSBoosted Trees	74.5	2900	4.6438

		Predicted		
		Careless	**Dangerous**	**Safe**
Actual	False Discovery Rate	1%	4%	8%
	Careless	**99%**	0%	1%
	Dangerous	0%	**96%**	4%
	Safe	1%	0%	**92%**

Figure 10: Confusion matrix showing the predicted and actual classifications of safe, careless, and dangerous driving. Values represent percentages. The False Discovery Rate row indicates the percentage of incorrect predictions for each predicted class. Diagonal cells (highlighted in green) represent correct classifications: 99% for careless, 96% for dangerous, and 92% for safe.

and +300 shows an optimal configuration for the proposed framework when employing ML variants. shows that the fitted line's intercept and slope values are projections for the distribution's position and residual parameters, respectively. Linear discriminant in (b) depicts the shortest training time of 3.5265. This means that this algorithm is able to train a model to classify data points into different categories more quickly than the other algorithms being compared. The y-axis of the graph shows the percentage accuracy of the different algorithms. The sample variance, which is a measure of the spread of the data, is being used to approximate the accuracy, prediction time, and training time obtained using several ML algorithms. The residual values in (c) y-axis show that the prediction was exceedingly low. Fitted values (refer to the x-axis) show that the prediction was significantly accurate; 0 on the y-axis indicates a 100% correct positive rate.

5.2.2. Kruskal-Wallis Results

The Kruskal-Wallis rank test was used to evaluate the algorithms and the results were presented in 13. The authors observed that the ensemble learning method with the Bagged model had the highest mean rank of 21 compared to the other variants of that model and other state-of-the-art ML algorithms. This suggests that the Bagged model's complex fitness function helped to extract rich feature vectors for classification. On the other hand, the Boosted Trees model had the highest mean rank of 21 compared to the other variants of that model and other state-of-the-art ML algorithms. However, the authors noted that this model's linear fitness function helps to extract poor feature vectors for classification. Additionally, the authors found

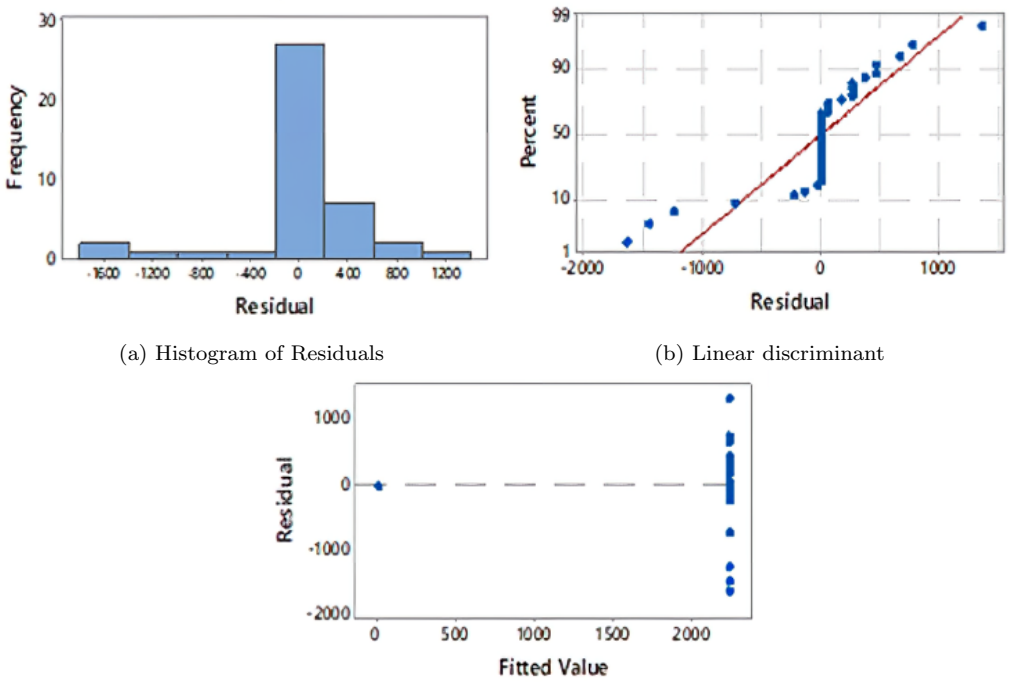

(a) Histogram of Residuals

(b) Linear discriminant

(c) Approximate Variance Inflation Factor

Figure 11: Residual Plots for Prediction Speed (obs/sec) vs Training Time (sec).

that the linear discriminant variant had the lowest mean rank of 1 in training time and achieved 90% accuracy. This algorithm used linear functions to evaluate the previous severity score and the expected total severity score of the following video frame. Finally, the authors noted that Gaussian Nïve Bayes was the second-best algorithm in terms of performance compared to others, except for bounded trees. This algorithm had an average mean rank of 20, achieved 93.2% accuracy, and had a z-score of 1.49. Overall, the results suggest that the Bagged model and Gaussian Nïve Bayes performed well in this experiment, while the Boosted Trees model may not be the best option for feature extraction in classification tasks.

5.2.3. Comparison of Models

The graph in Figure 12 compares the accuracy value of the proposed MDDRA, the work of Mengtao Zhu et al. [72], the work proposed by Yanli Ma et al. [73], and the work of Tianchi Liu et al. [74]. It can be seen that the proposed model has outperformed the current state-of-the-art in multi-

Table 13: Kruskal- Wallis ranks for the ML Algorithms to confirm Accuracy (α), Training Time (τ_T), and Prediction Time (τ_P), Z-Score (ζ), and the median value (μ).

Model	**Kruskal-Wallis Average Ranks**				
	$\boldsymbol{\mu}$	$\boldsymbol{\alpha}$	$\boldsymbol{\tau_P}$	$\boldsymbol{\tau_T}$	$\boldsymbol{\zeta}$
Bagged Trees	96.2	21	3	19	1.65
Boosted Trees	58.6	1.5	21	8	-1.57
Coarse Gaussian SVM	77.2	6	9	15	-0.83
Cubic SVM	92.4	18	9	10	1.16
Fine Gaussian SVM	58.6	1.5	7	17	-1.57
Fine KNN	79.1	8	17.5	6	-0.5
Gaussian Nïve Bayes	93.2	20	20	13	1.49
Kernel Nïve Bayes	90.1	14	4	18	0.5
KNN Coarse	59.3	3	13.5	7	-1.32
KNN Cosine	80.6	10.5	16	5	-0.08
KNN Cubic	76.4	5	5	4	-0.99
KNN Weighted KNN	80.6	10.5	13.5	3	-0.08
Linear Discriminant	90.9	15	17.5	1	0.66
Linear SVM	92	16	11	12	0.83
Medium Gaussian SVM	85.2	13	6	16	0.33
Medium KNN	78.3	7	13.5	2	-0.66
Quadratic Discriminant	82.9	12	13.5	14	0.17
Quadratic SVM	92.4	18	9	11	1.16
RUSBoosted Trees	74.5	4	19	9	-1.16
Subspace Discriminant	92.4	18	2	21	1.16
Subspace KNN	79.8	9	1	20	-0.33

class distraction prediction. Moreover, the model has achieved an accuracy of 96.21%, while the current state-of-the-art claims an accuracy of 95.87%, which is lower than our proposed methodology. Although Tianchi Liu et al. [74] have achieved slightly higher accuracy, they have worked on a binary classification problem. The multiclass classification is a more complex task than a simple binary classification model, the state-of-the-art model with excellent results in more than eight classes. Furthermore, the proposed model has provided fast results as high as 3600 observations per second, making the proposed model accurate but robust in terms of speed.

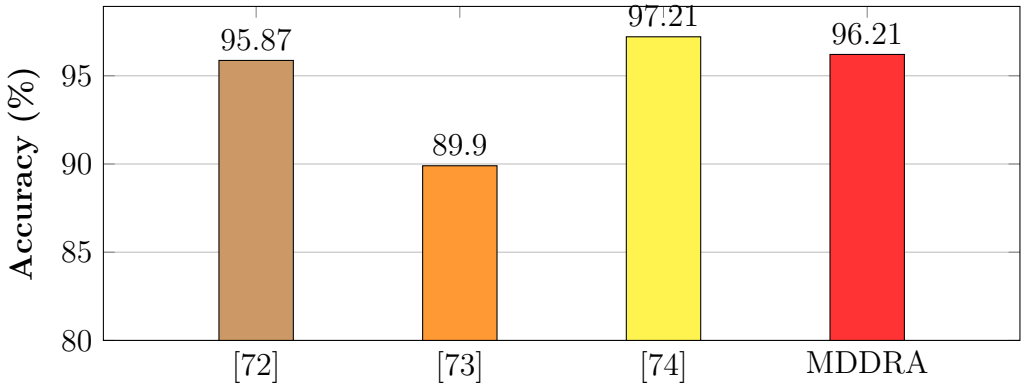

Figure 12: Accuracy in % Model comparison

This paper deals with the problem by employing machine learning. The authors have proposed a novel and robust MDDRA model. The model has tackled the driver with almost possible variants, such as the current state of the hand, which means whether the driver uses double hands, single hands, or no hands. Similarly, the type of road on which the vehicle is running, the face orientation on the road or off-road, whether it is a day or night, the eye gaze of the driver, if the weather is dry, rainy or snowy, what is a current manoeuvre, the surrounding vehicles, speed of the vehicle, speed of the surrounding vehicle, and pedestrians. The suggested model, MDDRA, considers vehicle, driver, and environmental data that occur during a journey to categorise drivers into a risk matrix such as safe, careless, and dangerous. The proposed model offers the flexibility to adjust parameters and weights to consider each event at a specific severity level. Real-world data was collected using the TeleFOT, which consisted of drivers using the same routes in the East Midlands, UK. The results have great potential to reduce road

accidents caused by distracted drivers. We have also tested the correlation of driver distraction (in-vehicle, vehicle, and environment distractions) on severity classification against the continuous driver distraction severity score. Furthermore, we have applied several machine learning techniques to classify and predict driver distraction according to severity levels to help transition from driver to vehicle. We implemented different ML models such as Discriminant, Nïve Bayes, SVM, and K-Means Nearest Neighbour (KNN) Ensemble ML for classification. Figure 13 shows the comparison of accuracy by applying these models. It can be seen that the Bagged Trees-based Ensemble model has provided the highest accuracy of 96.2% for classification, while fine Gaussian SVM and Boosted Trees-based ensemble methods have resulted in the lowest accuracy of 58.6% for the classification task. The comparison of various ML models is shown in Figure 13.

6. Conclusions

For a robust false proof alert system, the precise classification of driving behaviour is needed. However, to the best of our knowledge, the current work lacks complexity, rigidity, a synthesised dataset, more focus on a particular side of perspective (vehicle, driver, or environment), false positive classes, and low accuracy. This paper aimed to provide a novel MDDRA model that considers vehicle, driver, and environmental data during a trip to categorise the driver in a risk matrix as safe, careless, or dangerous. The MDDRA model offers flexibility in adjusting the parameters and weights to consider each event on a specific severity level. Real-world data was collected using the TeleFOT, consisting of drivers using the same routes in the East Midlands, UK. The results showed that it is possible to reduce road accidents caused by distracted drivers. We also tested the correlation between distraction (driver, vehicle, and environment) and classification severity based on a continuous distraction severity score.

Furthermore, we applied machine learning techniques to classify and predict driver distraction according to severity levels to aid the transition of control from the driver to the vehicle (vehicle takeover) when a situation is deemed risky. The experimental results obtained using various ML algorithms have shown better results than those of the baseline and the previous literature. The algorithm with the best performance was Ensemble Bagged Trees, which gave an accuracy of 96.2 %. However, this approach's limitation is that deep learning will produce better results regarding speed performance

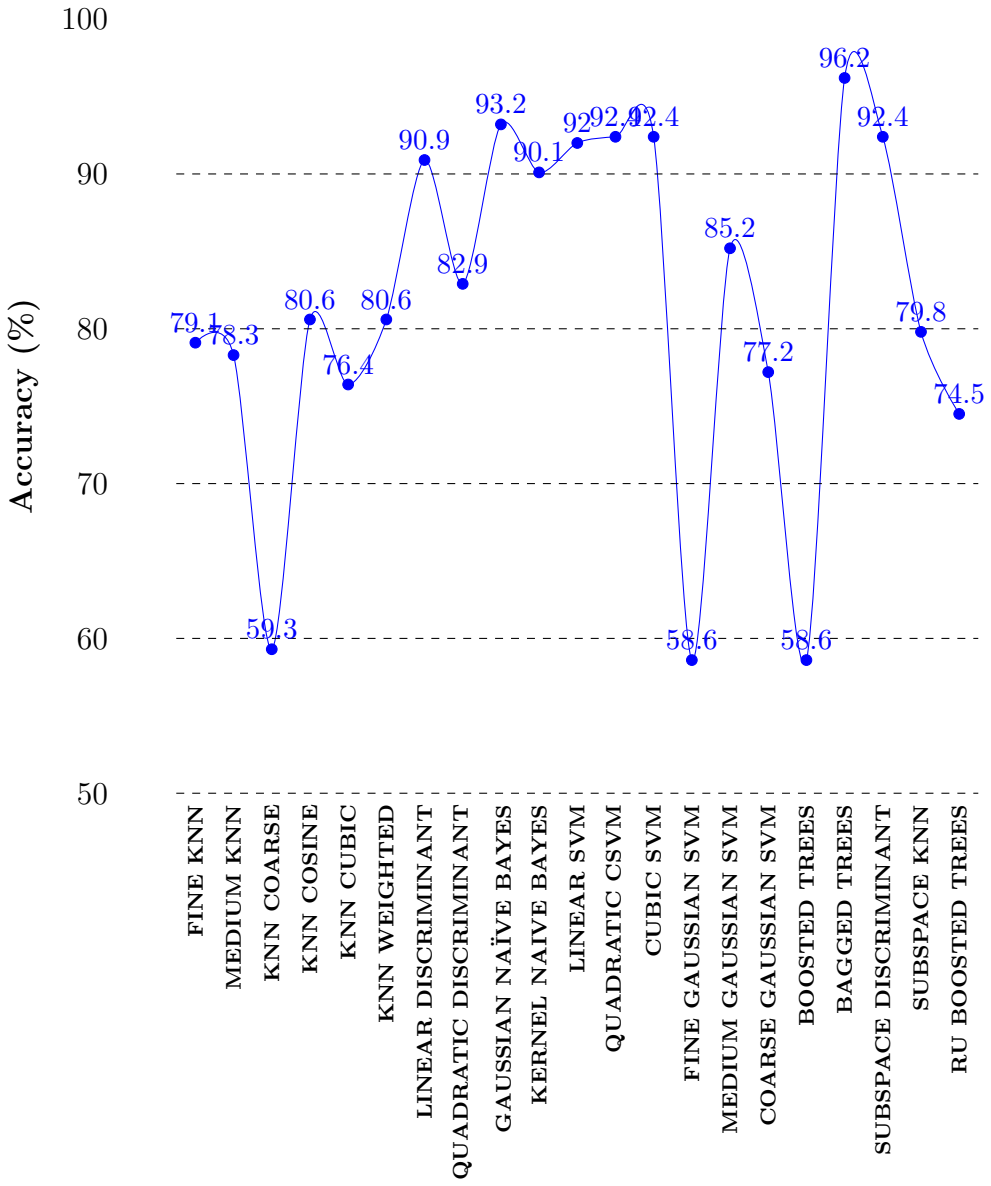

Figure 13: Accuracy across multiple ML models

than an ML technique. The result of the vehicle regression analysis had a higher degree of correlation and was highly significant. The MDDRA model can be adjusted to fit any distraction risk assessment considering the driver, vehicle, and environmental contexts. When assigning weights to pedestrians

on the road, we did not consider accidents or vehicles that hit pedestrians. However, the results of the regression show that vehicle distraction constitutes a higher level of significance. Factors such as sample size and data spread may have influenced the regression analysis's P-value results. Confidence intervals around the sample statistics would yield a better result than P-values alone. In addition, CNN-DBN-LSTM techniques in detecting and classifying multiclass driver distraction would yield more effective and efficient results. Finally, considering the accuracy over time complexity, the best ML model adopted is the Bagged Trees.

7. Acknowledgments

This research was supported by multiple higher education institutions. For the purpose of Open Access, the authors have applied a CC BY license to any Author Accepted Manuscript (AAM) version arising from this submission.

References

[1] "ADAS — Mobility and transport." `https://ec.europa.eu/transport/road/safety/users/young-people/distraction` (accessed May 25, 2021).

[2] A. S. Kulkarni and S. B. Shinde, "A review paper on monitoring driver distraction in real time using computer vision system", in Proceedings - 2017 IEEE International Conference on Electrical, Instrumentation and Communication Engineering, ICEICE 2017, 2017, vol. 2017-Decem, pp. 1–4, doi: 10.1109/ICEICE.2017.8191851.

[3] R. R. Herrera, C. Holloway, D. Z. Morgado Ramirez, B. Zhang, and Y. Cho, "Breathing Biofeedback Relaxation Intervention for Wheelchair Users in City Navigation," in Proceedings of the Annual International Conference of the IEEE Engineering in Medicine and Biology Society, EMBS, 2020, vol. 2020-July, pp. 4575–4578, doi: 10.1109/EMBC44109.2020.9176144.

[4] P. Ventsislavova and D. Crundall, "The hazard prediction test: A comparison of free-response and multiple-choice formats," Saf. Sci., vol. 109, pp. 246–255, 2018, doi: 10.1016/j.ssci.2018.06.004.

[5] T. M. Senserrick, M. J. Kallan, and F. K. Winston, "Child passenger injury risk in sibling versus non-sibling teen driver crashes: A US study," Inj. Prev., vol. 13, no. 3, pp. 207–210, Jun. 2007, doi: 10.1136/ip.2006.014332.

[6] C. A. R. Insurance, C. A. R. I. Claims, and B. Y. E. Delbridge, "Causes and Effects of Distracted Driving," pp. 1–10, 2020, Accessed: May 25, 2021. [Online]. Available: https://www.liveabout.com/causes-and-consequences-of-distracted-driving-527085.

[7] T. Choudhari and A. Maji, "Risk Assessment of Horizontal Curves Based on Lateral Acceleration Index: A Driving Simulator-Based Study," Transp. Dev. Econ., vol. 7, no. 1, pp. 1–11, Apr. 2021, doi: 10.1007/s40890-020-00111-2.

[8] N. Kinnear and A. Stevens, "The battle for attention Driver distraction - a review of recent research and knowledge," 2015, Accessed: May 25, 2021. [Online]. Available: https://trid.trb.org/view/1377052.

[9] C. Li, S. H. Chan, and Y. T. Chen, "Who make drivers stop? Towards driver-centric risk assessment: Risk object identification via causal inference," in IEEE International Conference on Intelligent Robots and Systems, Oct. 2020, pp. 10711–10718, doi: 10.1109/IROS45743.2020.9341072.

[10] J. Michaels et al., "Driving simulator scenarios and measures to faithfully evaluate risky driving behavior: A comparative study of different driver age groups," PLoS One, vol. 12, no. 10, Oct. 2017, doi: 10.1371/journal.pone.0185909.

[11] J. Liu, F. Jin, Q. Xie, and M. Skitmore, "Improving risk assessment in financial feasibility of international engineering projects: A risk driver perspective," Int. J. Proj. Manag., vol. 35, no. 2, pp. 204–211, 2017, doi: 10.1016/j.ijproman.2016.11.004.

[12] J. L. Yin and B. H. Chen, "An Advanced Driver Risk Measurement System for Usage-Based Insurance on Big Driving Data," IEEE Trans. Intell. Veh., vol. 3, no. 4, pp. 585–594, 2018, doi: 10.1109/TIV.2018.2874530.

[13] H. Mao, F. Guo, X. Deng, and Z. R. Doerzaph, "Decision-adjusted driver risk predictive models using kinematics information," Accid. Anal. Prev., vol. 156, 2021, doi: 10.1016/j.aap.2021.106088.

[14] A. Tefferi and A. M. Vannucchi, "Genetic Risk Assessment in Myeloproliferative Neoplasms," Mayo Clinic Proceedings, vol. 92, no. 8. pp. 1283–1290, 2017, doi: 10.1016/j.mayocp.2017.06.002.

[15] J. D. Paradis, "Reporting on risk: A journalist's handbook on environmental risk assessment," J. Crim. Justice, vol. 23, no. 4, p. 391, 1995, doi: 10.1016/0047-2352(95)90043-8.

[16] K. Berdica, "An introduction to road vulnerability: What has been done, is done and should be done," Transp. Policy, vol. 9, no. 2, pp. 117–127, 2002, doi: 10.1016/S0967-070X(02)00011-2.

[17] K. Berdica and L. G. Mattsson, "Vulnerability: A model-based case study of the road network in Stockholm," in Advances in Spatial Science, no. 9783540680550, Springer International Publishing, 2007, pp. 81–106.

[18] W. ElDessouki, J. Ivan, and E. Anagnostou, "Using relative risk analysis to improve connecticut freeway traffic safety under adverse weather conditions," 2004. Accessed: May 25, 2021. [Online]. Available: https://books.google.com.pk/books/about/Using_Relative_Risk_Analysis_to_Improve.html?id=VfjrdElzZxEC&redir_esc=y

[19] X. Cai, C. Wang, S. Chen, and J. Lu, "Model development for risk assessment of driving on freeway under rainy weather conditions," PLoS One, vol. 11, no. 2, Feb. 2016, doi: 10.1371/journal.pone.0149442.

[20] C. Dong, C. C. Loy, K. He, and X. Tang, "Image Super-Resolution Using Deep Convolutional Networks," IEEE Trans. Pattern Anal. Mach. Intell., vol. 38, no. 2, pp. 295–307, 2016, doi: 10.1109/TPAMI.2015.2439281.

[21] Z. Hu, N. Uchida, Y. Wang, and Y. Dong, "Face orientation estimation for driver monitoring with a single depth camera," in IEEE Intelligent Vehicles Symposium, Proceedings, Aug. 2015, vol. 2015-Augus, pp. 958–963, doi: 10.1109/IVS.2015.7225808.

[22] K. Sato, M. Ito, H. Madokoro, and S. Kadowaki, "Driver body information analysis for distraction state detection," in 2015 IEEE International Conference on Vehicular Electronics and Safety, ICVES 2015, Feb. 2016, pp. 13–18, doi: 10.1109/ICVES.2015.7396886.

[23] A. Rasouli, I. Kotseruba, and J. K. Tsotsos, "Understanding Pedestrian Behavior in Complex Traffic Scenes," IEEE Trans. Intell. Veh., vol. 3, no. 1, pp. 61–70, Mar. 2018, doi: 10.1109/TIV.2017.2788193.

[24] A. Fasanmade et al., "A Fuzzy-Logic Approach to Dynamic Bayesian Severity Level Classification of Driver Distraction Using Image Recognition," IEEE Access, vol. 8, pp. 95197–95207, 2020, doi: 10.1109/ACCESS.2020.2994811.

[25] N. Das, E. Ohn-Bar, and M. M. Trivedi, "On Performance Evaluation of Driver Hand Detection Algorithms: Challenges, Dataset, and Metrics," in IEEE Conference on Intelligent Transportation Systems, Proceedings, ITSC, 2015, vol. 2015-Octob, pp. 2953–2958, doi: 10.1109/ITSC.2015.473.

[26] C. Dong, C. C. Loy, K. He, and X. Tang, "Learning a deep convolutional network for image super-resolution," in Lecture Notes in Computer Science (including subseries Lecture Notes in Artificial Intelligence and Lecture Notes in Bioinformatics), 2014, vol. 8692 LNCS, no. PART 4, pp. 184–199, doi: 10.1007/978-3-319-10593-2_13.

[27] T. H. N. Le, C. Zhu, Y. Zheng, K. Luu, and M. Savvides, "Robust hand detection in Vehicles," in Proceedings - International Conference on Pattern Recognition, Jan. 2016, vol. 0, pp. 573–578, doi: 10.1109/ICPR.2016.7899695.

[28] T. H. N. Le, K. G. Quach, C. Zhu, C. N. Duong, K. Luu, and M. Savvides, "Robust Hand Detection and Classification in Vehicles and in the Wild," in IEEE Computer Society Conference on Computer Vision and Pattern Recognition Workshops, 2017, vol. 2017-July, pp. 1203–1210, doi: 10.1109/CVPRW.2017.159.

[29] B. Kapitaniak, M. Walczak, M. Kosobudzki, Z. Jóźwiak, and A. Bortkiewicz, "Application of eye-tracking in drivers testing: A review of research," International Journal of Occupational Medicine

and Environmental Health, vol. 28, no. 6. pp. 941–954, 2015, doi: 10.13075/ijomeh.1896.00317.

[30] W. Yuan, Z. Liu, and R. Fu, "Predicting drivers' eyes-off-road duration in different driving scenarios," Discret. Dyn. Nat. Soc., vol. 2018, 2018, doi: 10.1155/2018/3481628.

[31] B. G. Simons-Morton, F. Guo, S. G. Klauer, J. P. Ehsani, and A. K. Pradhan, "Keep your eyes on the road: Young driver crash risk increases according to duration of distraction," J. Adolesc. Heal., vol. 54, no. 5 SUPPL., pp. S61–S67, 2014, doi: 10.1016/j.jadohealth.2013.11.021.

[32] P. Doshi, D. Kapur, R. Iyer, and A. Chatterjee, "Smart mobility: Algorithm for road and driver type determination," in 2017 IEEE Transportation Electrification Conference, ITEC-India 2017, Apr. 2018, vol. 2018-Janua, pp. 1–4, doi: 10.1109/ITEC-India.2017.8333895.

[33] C. Chai, R. Zhao, J. Shi, J. Zhou, and Z. Yang, "The effect of road environment and type of vehicles on road rage in China," in Proceedings - 2019 12th International Symposium on Computational Intelligence and Design, ISCID 2019, 2019, pp. 200–203, doi: 10.1109/ISCID.2019.10129.

[34] J. E. Meseguer, C. T. Calafate, J. C. Cano, and P. Manzoni, "DrivingStyles: A smartphone application to assess driver behavior," in Proceedings - International Symposium on Computers and Communications, 2013, pp. 535–540, doi: 10.1109/ISCC.2013.6755001.

[35] A. Rakotonirainy, "Design of context-aware systems for vehicles using complex system paradigms," in CEUR Workshop Proceedings, 2005, vol. 158, Accessed: May 25, 2021. [Online]. Available: http://eprints.qut.edu.au.

[36] I. Khan and S. Khusro, "Towards the Design of Context-Aware Adaptive User Interfaces to Minimize Drivers' Distractions," Mob. Inf. Syst., vol. 2020, 2020, doi: 10.1155/2020/8858886.

[37] X. Jianfeng, G. Hongyu, T. Jian, L. Liu, and L. Haizhu, "A classification and recognition model for the severity of road traffic accident," Eco-Mobility Futur. Cities-Research Artic. Adv. Mech. Eng., vol. 11, no. 5, pp. 1–8, May 2019, doi: 10.1177/1687814019851893.

[38] F. Malin, I. Norros, and S. Innamaa, "Accident risk of road and weather conditions on different road types," Accid. Anal. Prev., vol. 122, pp. 181–188, Jan. 2019, doi: 10.1016/j.aap.2018.10.014.

[39] L. A. Sherretz and B. C. Farhar, "An Analysis of the Relationship Between Rainfall and the Occurrence Of Traffic Accidents," J. Appl. Meteorol., vol. 17, no. 5, pp. 711–715, 1978, doi: 10.1175/1520-0450(1978)017¡0711:aaotrb¿2.0.co;2.

[40] R. Bergel-Hayat, M. Debbarh, C. Antoniou, and G. Yannis, "Explaining the road accident risk: Weather effects," Accid. Anal. Prev., vol. 60, pp. 456–465, 2013, doi: 10.1016/j.aap.2013.03.006.

[41] H. Brodsky and A. S. Hakkert, "Risk of a road accident in rainy weather," Accid. Anal. Prev., vol. 20, no. 3, pp. 161–176, 1988, doi: 10.1016/0001-4575(88)90001-2.

[42] J. Andrey and B. Mills, Collisions, casualties and costs: weathering the elements on Canadian roads, no. 33. 2003.

[43] "2-Second Rule for Distracted Driving Can Mean Life or Death - The New York Times." https://www.nytimes.com/2018/09/27/business/distracted-driving-auto-industry.html (accessed May 25, 2021).

[44] C. Wu, D. Yu, A. Doherty, T. Zhang, L. Kust, and G. Luo, "An investigation of perceived vehicle speed from a driver's perspective," PLoS One, vol. 12, no. 10, Oct. 2017, doi: 10.1371/journal.pone.0185347.

[45] E. de Bellis, M. Schulte-Mecklenbeck, W. Brucks, A. Herrmann, and R. Hertwig, "Blind haste: As light decreases, speeding increases," PLoS One, vol. 13, no. 1, Jan. 2018, doi: 10.1371/journal.pone.0188951.

[46] Predictive Modeling and Analysis of Monkeypox Outbreaks Using Machine Learning Techniques (R. M. . Maher, S. H. . Rashid, M. A. Habeeb, Y. L. . Khaleel, & F. N. . Ameen , Trans.). (2025). Applied Data Science and Analysis, 2025, 94-111. https://doi.org/10.58496/ADSA/2025/006

[47] A. Bener, T. Özkan, and T. Lajunen, "The Driver Behaviour Questionnaire in Arab Gulf countries: Qatar and United Arab Emirates," Accid. Anal. Prev., vol. 40, no. 4, pp. 1411–1417, 2008, doi: 10.1016/j.aap.2008.03.003.

[48] A. Mishra and P. Bajaj, "Driver's Behaviour Monitoring on Urban Roads of a Tier 2 City in India," in International Conference on Emerging Trends in Engineering and Technology, ICETET, Mar. 2016, vol. 2016-March, pp. 134–140, doi: 10.1109/ICETET.2015.13.

[49] A. Kumar and R. Patra, "Driver drowsiness monitoring system using visual behaviour and machine learning," in ISCAIE 2018 - 2018 IEEE Symposium on Computer Applications and Industrial Electronics, 2018, pp. 339–344, doi: 10.1109/ISCAIE.2018.8405495.

[50] E. S. Lee and D. Kum, "Feature-based lateral position estimation of surrounding vehicles using stereo vision," in IEEE Intelligent Vehicles Symposium, Proceedings, Jul. 2017, pp. 779–784, doi: 10.1109/IVS.2017.7995811.

[51] D. Xu, H. Zhao, F. Guillemard, S. Geronimi, and F. Aioun, "Scene-Aware driver state understanding in car-following behaviors," in IEEE Intelligent Vehicles Symposium, Proceedings, Jul. 2017, pp. 1490–1496, doi: 10.1109/IVS.2017.7995920.

[52] U. Mittal, R. Potnuru, and P. Chawla, "Vehicle Detection and Classification using Improved Faster Region Based Convolution Neural Network," in ICRITO 2020 - IEEE 8th International Conference on Reliability, Infocom Technologies and Optimization (Trends and Future Directions), 2020, pp. 511–514, doi: 10.1109/ICRITO48877.2020.9197805.

[53] J. Gong, J. Zhao, F. Li, and H. Zhang, "Vehicle detection in thermal images with an improved yolov3-tiny," in Proceedings of 2020 IEEE International Conference on Power, Intelligent Computing and Systems, ICPICS 2020, 2020, pp. 253–256, doi: 10.1109/ICPICS50287.2020.9201995.

[54] R. A. Kharjul, V. K. Tungar, Y. P. Kulkarni, S. K. Upadhyay, and R. Shirsath, "Real-Time pedestrian detection using SVM and AdaBoost," in International Conference on Energy Systems and Applications, ICESA 2015, 2016, pp. 740–743, doi: 10.1109/ICESA.2015.7503447.

[55] K. Tateiwa and K. Yamada, "Estimating driver awareness of pedestrians in crosswalk in the path of right or left turns at an intersection from

vehicle behavior," in IEEE Intelligent Vehicles Symposium, Proceedings, 2015, vol. 2015-Augus, pp. 952–957, doi: 10.1109/IVS.2015.7225807.

[56] K. Tateiwa, A. Nakamura, and K. Yamada, "Study on estimating driver awareness of pedestrians while turning right at intersection based on vehicle behavior utilizing driving simulator," in IEEE Intelligent Vehicles Symposium, Proceedings, 2016, vol. 2016-Augus, pp. 388–393, doi: 10.1109/IVS.2016.7535415.

[57] A. Rangesh, O. B. Eshed, K. Yuen, and M. M. Trivedi, "Pedestrians and their phones - Detecting phone-based activities of pedestrians for autonomous vehicles," in IEEE Conference on Intelligent Transportation Systems, Proceedings, ITSC, 2016, pp. 1882–1887, doi: 10.1109/ITSC.2016.7795861.

[58] P. Polack, F. Altche, B. DAndrea-Novel, and A. De La Fortelle, "The kinematic bicycle model: A consistent model for planning feasible trajectories for autonomous vehicles?," in IEEE Intelligent Vehicles Symposium, Proceedings, 2017, pp. 812–818, doi: 10.1109/IVS.2017.7995816.

[59] D. D. Clarke, P. Ward, C. Bartle, and W. Truman, "Young driver accidents in the UK: The influence of age, experience, and time of day," Accid. Anal. Prev., vol. 38, no. 5, pp. 871–878, Sep. 2006, doi: 10.1016/j.aap.2006.02.013.

[60] A. F. Williams, "Teenage drivers: Patterns of risk," in Journal of Safety Research, Jan. 2003, vol. 34, no. 1, pp. 5–15, doi: 10.1016/S0022-4375(02)00075-0.

[61] D. Sommer and M. Golz, "Evaluation of PERCLOS based current fatigue monitoring technologies," in 2010 Annual International Conference of the IEEE Engineering in Medicine and Biology Society, EMBC'10, 2010, pp. 4456–4459, doi: 10.1109/IEMBS.2010.5625960.

[62] H. Ginting, G. Näring, and E. S. Becker, "Attentional bias and anxiety in individuals with coronary heart disease," Psychol. Heal., vol. 28, no. 11, pp. 1306–1322, Nov. 2013, doi: 10.1080/08870446.2013.803554.

[63] O. Lopez-Fernandez, M. Freixa-Blanxart, and M. L. Honrubia-Serrano, "The problematic internet entertainment use scale for adolescents:

Prevalence of problem internet use in Spanish high school students," Cyberpsychology, Behav. Soc. Netw., vol. 16, no. 2, pp. 108–118, Feb. 2013, doi: 10.1089/cyber.2012.0250.

[64] G. B. Casal, J. Carlos, S. Normas, P. La, and D. E. C. Cl, "International Journal of Clinical and Health Psychology," International Journal of Clinical and Health Psychology, vol. 2, no. 1. pp. 525–532, 2002, Accessed: May 25, 2021. [Online].

[65] T. C. CHIVERS, W. J. ROGERS, and M. E. WILLIAMS, "A TECHNIQUE FOR THE MEASUREMENT OF GAS-LEAKAGE.," psycnet.apa.org. 1974, Accessed: May 25, 2021. [Online]. Available: https://psycnet.apa.org/record/1933-01885-001.

[66] C. León-Mantero, J. C. Casas-Rosal, C. Pedrosa-Jesús, and A. Maz-Machado, "Measuring attitude towards mathematics using Likert scale surveys: The weighted average," PLoS One, vol. 15, no. 10 October, Oct. 2020, doi: 10.1371/journal.pone.0239626.

[67] J. F. Liu, Y. F. Su, M. K. Ko, and P. N. Yu, "Development of a vision-based driver assistance system with lane departure warning and forward collision warning functions," in Proceedings - Digital Image Computing: Techniques and Applications, DICTA 2008, 2008, pp. 480–485, doi: 10.1109/DICTA.2008.78.

[68] "TeleFOT - UK DFOT3 - FOT-Net WIKI." https://wiki.fot-net.eu/index.php/TeleFOT_-_UK_DFOT3 (accessed May 25, 2021).

[69] M. M. Kunt, I. Aghayan, and N. Noii, "Prediction for traffic accident severity: Comparing the artificial neural network, genetic algorithm, combined genetic algorithm and pattern search methods," Transport, vol. 26, no. 4, pp. 353–366, Dec. 2011, doi: 10.3846/16484142.2011.635465.

[70] J. Morton, T. A. Wheeler, and M. J. Kochenderfer, "Analysis of Recurrent Neural Networks for Probabilistic Modeling of Driver Behavior," IEEE Trans. Intell. Transp. Syst., vol. 18, no. 5, pp. 1289–1298, 2017, doi: 10.1109/TITS.2016.2603007.

[71] Graph-Theoretic Characterizations of Quasi-Idempotents in Full Order-Preserving Transformation Semigroup (E. . C, A. . Imam, M. Balarabe,

& O. O. O , Trans.). (2025). Babylonian Journal of Mathematics, 2025, 88-91. https://doi.org/10.58496/BJM/2025/009

[72] M. Zhu, Y. Li, and Y. Wang, "Design and experiment verification of a novel analysis framework for recognition of driver injury patterns: From a multi-class classification perspective," Accid. Anal. Prev., vol. 120, pp. 152–164, Nov. 2018, doi: 10.1016/j.aap.2018.08.011.

[73] Y. Ma, G. Gu, B. Yin, S. Qi, K. Chen, and C. Chan, "Support vector machines for the identification of real-time driving distraction using in-vehicle information systems," J. Transp. Saf. Secur., 2020, doi: 10.1080/19439962.2020.1774019.

[74] T. Liu, Y. Yang, G. Bin Huang, Y. K. Yeo, and Z. Lin, "Driver Distraction Detection Using Semi-Supervised Machine Learning," IEEE Trans. Intell. Transp. Syst., vol. 17, no. 4, pp. 1108–1120, Apr. 2016, doi: 10.1109/TITS.2015.2496157.

[75] Carsten, O. M. J., & Brookhuis, K. (2005). Issues arising from the HASTE experiments. Transportation Research Part F: Traffic Psychology and Behaviour, 8(2), 191–196.

[76] Worood Esam Noori and A. S. Albahri (trans.) (2023) "Towards Trustworthy Myopia Detection: Integration Methodology of Deep Learning Approach, XAI Visualization, and User Interface System", Applied Data Science and Analysis, 2023, pp. 1–15. doi:10.58496/ADSA/2023/001.

[77] The Role of Artificial Intelligence in Early Tumor Detection: An XGBoost Risk Assessment Model for Egyptian Patients (T. . MZILI, M. Mzili, S. I. Bouderba, A. Abatal, W. Aribowo, & Z. Oughannou , Trans.). (2025). Mesopotamian Journal of Artificial Intelligence in Healthcare, 2025, 85-92. https://doi.org/10.58496/MJAIH/2025/008

[78] Adamopoulos, I., 2025. A Novel AI based Modeling with Bias Classification Hybrid Risk Evaluation System for Confidence Enhanced Network Meta Analysis of Occupational Hazards and Burnout Risk among Public Health Inspectors; Mesopotamian Journal of Artificial Intelligence in Healthcare, pp.219-233. https://doi.org/10.58496/MJAIH/2025/021

[79] Yass, W.G. and Faris, M. (trans.) (2023) "Integrating computer vision, web systems and embedded systems to develop an intelligent monitoring

system for violating vehicles", Babylonian Journal of Internet of Things, 2023, pp. 69–73. doi:10.58496/BJIoT/2023/009.

[80] Existence and Uniqueness Theorem of Multi-Dimensional Integro-Differential Equations With Fractional Differointegrations (Z. A. . Mohammed, M. . Damak, F. S. . Fadhel, & H. S. . Altahainah , Trans.). (2025). Babylonian Journal of Mathematics, 2025, 44-49. https://doi.org/10.58496/BJM/2025/006

[81] Abed, Saad Abbas; Ghassan, Mona; Latef, Shaimaa Qais; and Hassan, Hind S. (2025) "Reliability-Based Design Optimization Using Differential-Algebraic Equations," Iraqi Journal for Computer Science and Mathematics: Vol. 6: Iss. 3, Article 8. DOI: https://doi.org/10.52866/2788-7421.1280

[82] Reliability Allocation in Complex Systems Using Fuzzy Logic Modules (S. A. Abed & Z. H. Khalil , Trans.). (2023). Babylonian Journal of Mathematics, 2023, 78-83. https://doi.org/10.58496/BJM/2023/015

[83] Optimal Time Window Selection in the Wavelet Signal Domain for Brain–Computer Interfaces in Wheelchair Steering Control (Z. Al-Qaysi, M. S. Suzani, N. bin Abdul Rashid, R. A. Aljanabi, R. D. Ismail, M. Ahmed, W. A. W. Sulaiman, & H. Kumar , Trans.). (2024). Applied Data Science and Analysis, 2024, 69-81. https://doi.org/10.58496/ADSA/2024/007